Selected Novel Technologies for Licensing

2012 MRS Fall

Innovative Materials for your Products

Devices

Advanced Materials

Oxide

Carbon

Metal

Soft Material

Measuring Equipment

Japan Science and Technology Agency

Devices

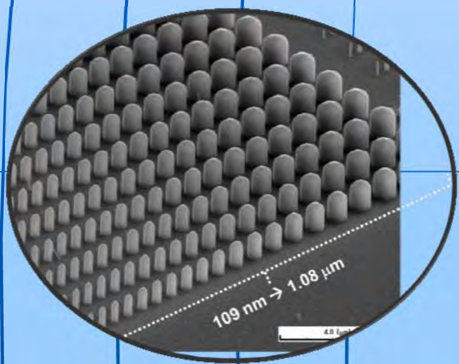
109 nm → 1.08 μm

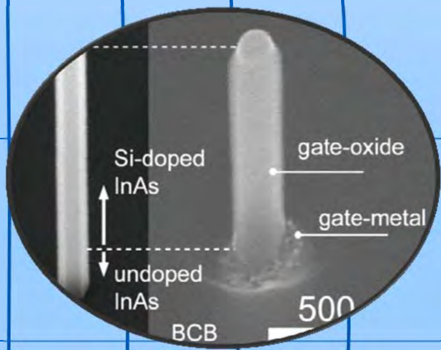
Si-doped
InAs
gate-oxide
gate-metal
undoped
InAs
BCB
500

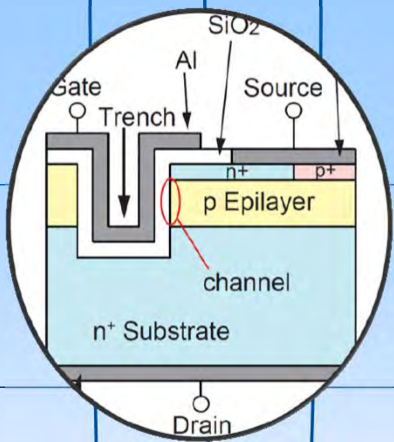
SiO2
Al
Gate
Source
Trench
n+
p+
p Epilayer
channel
n+ Substrate
Drain

Growth of InGaN/GaN Nanocolumn Arrays and their LEDs

Prof. Katsumi KISHINO & Associate Prof. Akihiko KIKUCHI (Sophia University)

1. Growth of InGaN/GaN Nanocolumn Arrays

- We found a regularly arranged InGaN/GaN nanocolumn array is fabricated using Ti-mask selective-area growth (i.e. Ti-nanohole-patterned GaN templates on sapphire substrate) by RF-plasma-assisted MBE.

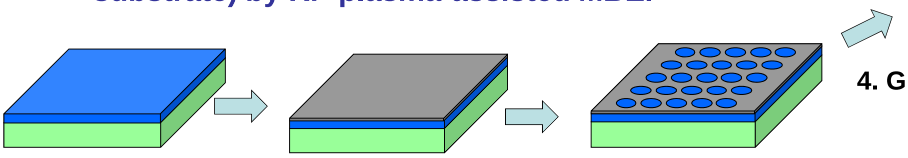

1. MOVPE-GaN template (3.5μm)
2. Ti thin film deposition
3. make Ti nano-hole by FIB technique

Period: 400, 600 nm
Hole size: ~150 nm

4. Growth of InGaN/GaN nanocolumn

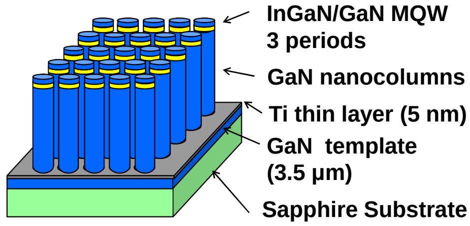

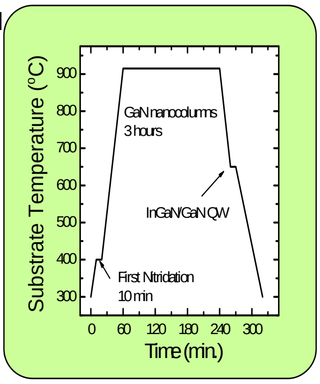

2. Crystallinity Control by Nanocolumn Diameter

- Fabrication Control of Nanocolumn Diameter

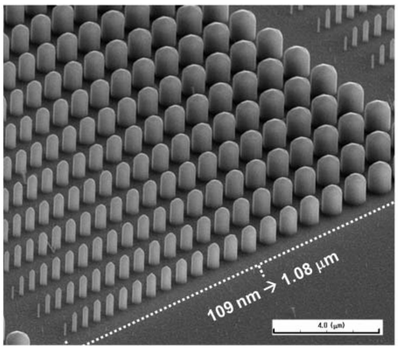

- Dislocation density is minimized in nanocolumn of less than 250nm diameter

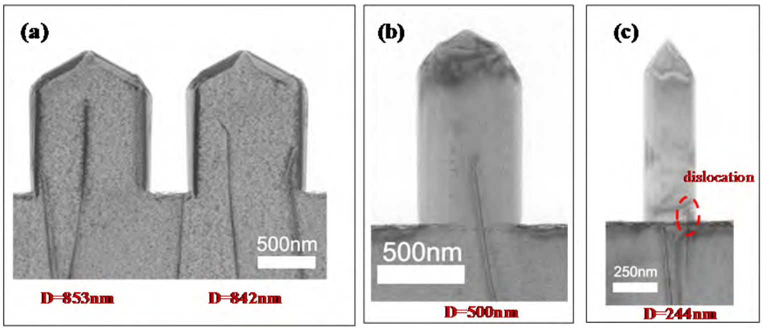

3. Fabrication of Nanocolumn LED

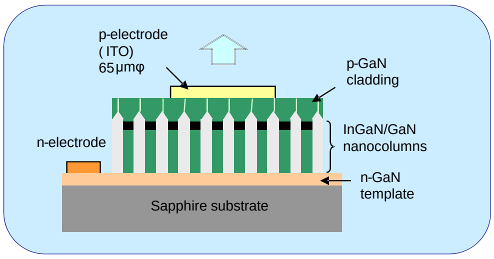

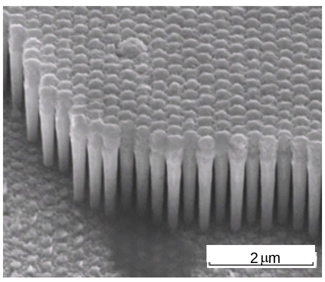

ITO electrode
p-type GaN cladding
p-type AlGaN EBL (10nm thick)
InGaN(3nm)/GaN(12nm) MQW (3-period)
InGaN(1.5nm)/GaN(1.5nm) superlattice (25- period)

- Green LED of nanocolumn InGaN/GaN arrays shows a higher PL efficiency which means good crystallinity of the arrays.

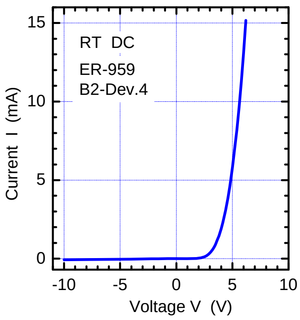

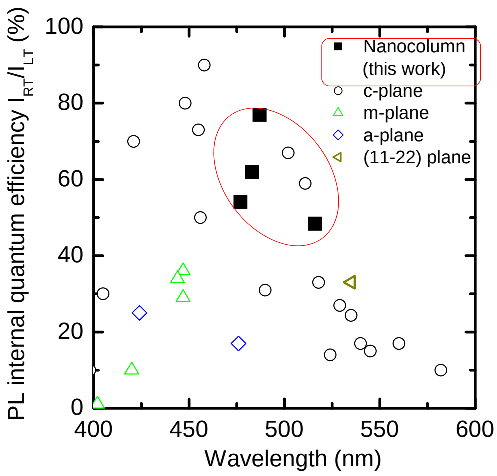

PL efficiencies as a function of peak wavelength

4. Patent available for licensing

Patent No. : WO/2009/031276,WO2009/069286, WO/2010/023921 (JP,US,EP,KR,CN,TW)

Contact : Masaru OZAKI (JST)
phone:+81-3-5214-8486, e-mail: license@jst.go.jp

Steep-Slope Tunnel Field-Effect Transistor (FET) using III-V Nanowire on Si

Prof. Takashi FUKUI & Dr. Katsuhiro TOMIOKA (Hokkaido University)

- As the scaling of Si transistors is reaching its limit, they are expected to have new gate architectures, channel materials and switching mechanisms which have both high integration and low power consumption.
- Our tunnel FET is a next generation transistor exceeding the limit of Si transistors.

1. Epitaxial Growth of III-V Nanowire on Si

- Tunnel FET has not been achieved because narrow band gap III-V/Si is a highly mismatched system.

- Selective area growth brings epitaxial III-V nanowire on Si (111) substrate

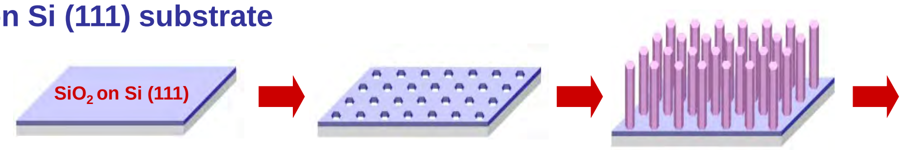

SiO_2 thermal oxidation → EB lithography and etching → MOVPE growth of InAs or GaAs or InGaAs

Hole Pitch of 0.4 ~ 3μm
Hole Diameter (d) of 20 ~ 200nm

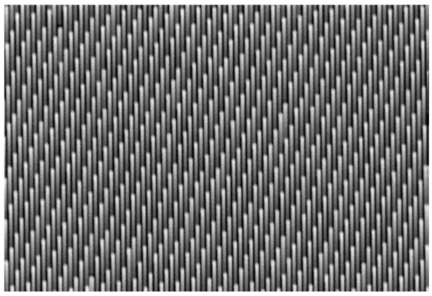

2. Device Structure of Vertical Tunnel FET

30º-tilted view of SEM image

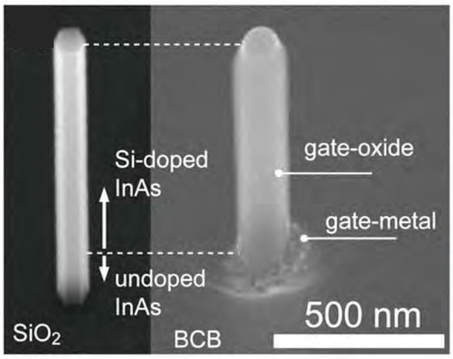

Device schematic

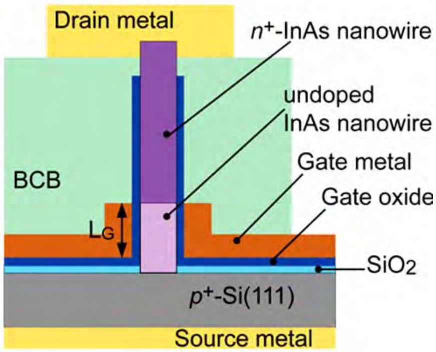

Nanowire : 80 nm in diameter
1.4 μm in height

Source (S) : p^+-Si => Ground
($p \sim 1\times10^{19}$ cm^{-3})
Gate (G) : undoped InAs region
($n \sim 10^{17}$ cm^{-3})
Drain (D) : n^+-InAs region ($n \sim 10^{19}$ cm^{-3})

3. High Performance of Vertical Tunnel FET

- The combination of a narrow band gap III-V with Si is a good system for boosting up the ON-state current and has high band-to-band tunneling efficiency.

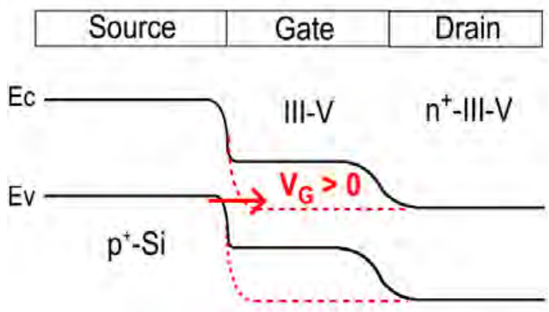

- Very steep turn-on switching was observed. The subthreshold slope (SS) is far lower value than 60mV/dec.(theoretical limit value) of Si FET.

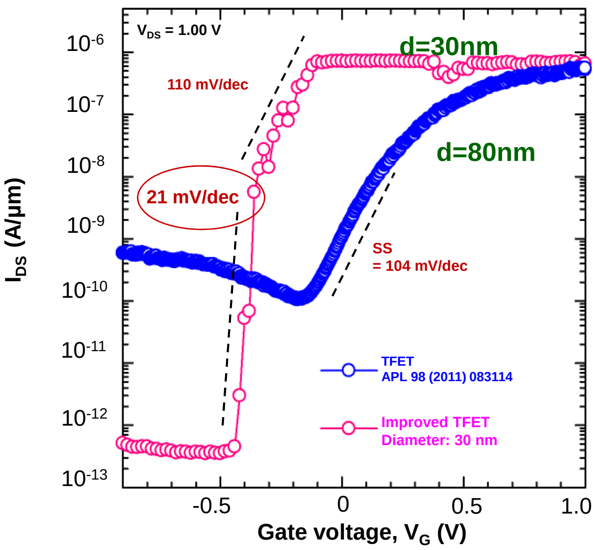

SS: 21 mV/dec (~4dec.)
I_{ON} / I_{OFF}: ~ 10^6
I_{ON} : 0.9 μA/μm @ V_{DS} = 1.0 V

4. Patent available for licensing

Patent No. : WO/2011/040012
(JP,US,EP,KR,CN)

Contact : Masaru OZAKI (JST)
phone: +81-3-5214-8486
e-mail: license@jst.go.jp

4H-SiC MOSFETs with High Channel Mobility by P-Doped Gate Oxide

Assistant Prof. Hiroshi YANO (NAIST)

1. 4H-SiC MOSFET

- Expected as ultra-low power loss devices
- Typical channel mobility obtained by nitridation, NO or N_2O annealing, was 20-40 cm^2/Vs.
  Low channel mobility is a big issue!
- We need to make efforts to find other techniques.

P-doped Gate oxide by $POCl_3$ annealing reduces D_{it} ($< 1 \times 10^{11}$ $cm^{-2}eV^{-1}$) and improves channel mobility ($\sim$ 100 $cm^2/Vsec$).

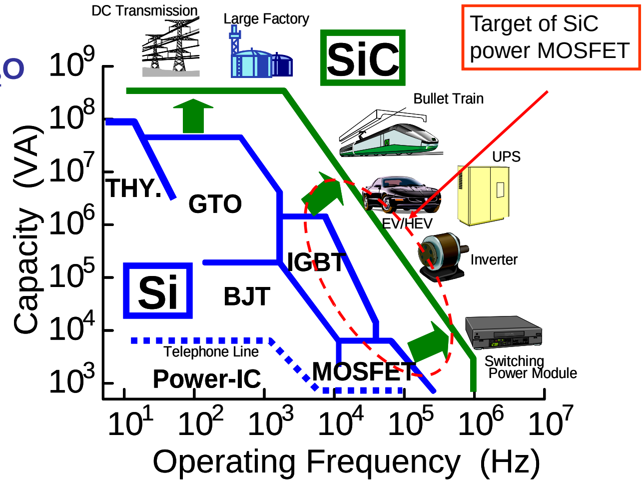

2. Device Fabrication with P-Doped Gate SiO_2

(0001) Si-face 4H-SiC
- Dry oxidation (t_{ox}~ 55 nm) ; 1200 °C, 160 min
- $POCl_3$ anneal ; 1000 °C, 10 min
- N_2 anneal ; 1000 °C, 30 min
- Al electrode evaporation
- N_2 PMA ; 400 °C, 30 min

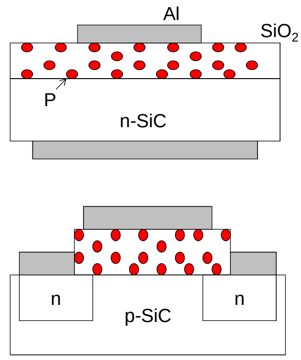

N-MOS Capacitor (Gate diameter=300µm)

N-Channel MOSFET (Channel length/Width =30/200µm)

3. MOSFET Performance with P-doped Oxide Gate

- D_{it} can be reduced by $POCl_3$ anneal
- High field-effect mobility, $\mu_{FE,max}$ = 89 cm^2/Vs

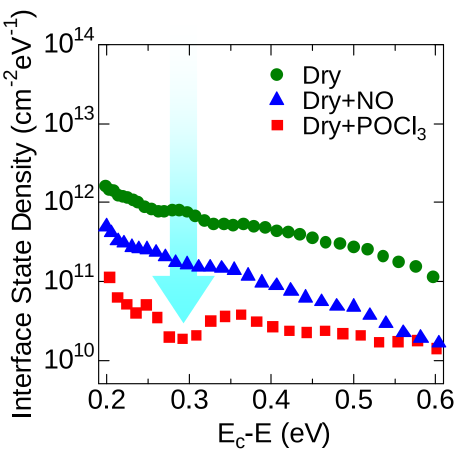

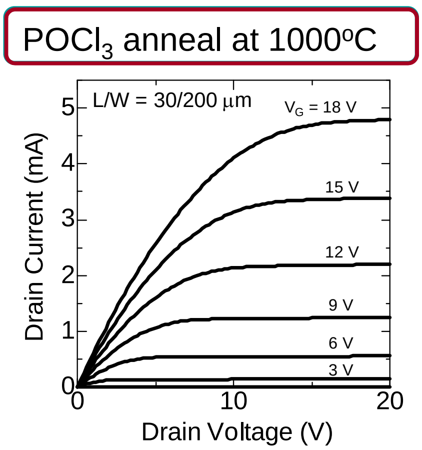

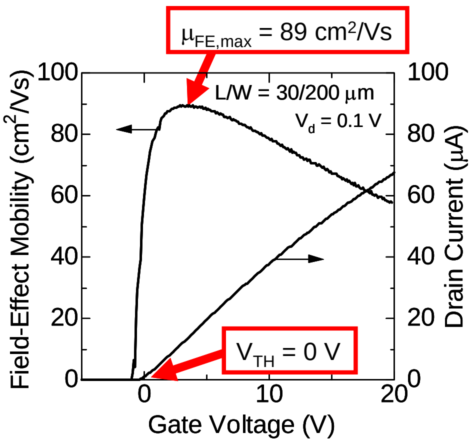

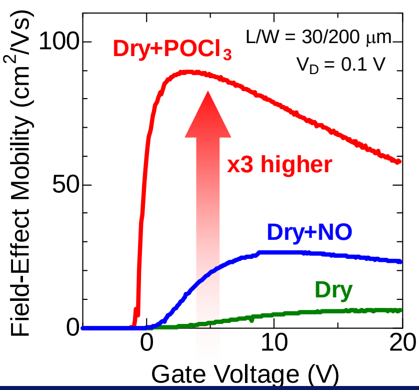

4. Patent available for licensing

Patent No. : WO/2011/074237 (JP,US,EP,KR,CN)

Contact : Masaru OZAKI (JST)
phone: +81-3-5214-8486
e-mail: license@jst.go.jp

4H-SiC Trench MOSFETs with High Channel Mobility by using Tilted Trench Sidewalls

Assistant Prof. Hiroshi YANO (NAIST)

1. Trench MOSFET

- Trench MOSFET is a favorable structure to achieve low on-resistance because of reasons below.
  - Channel on-trench sidewall
  - High channel density
  - No JFET (Junction Field Effect Transistor) region
  - Use of $(11\bar{2}0)$ face

  → Low on-resistance

Off-angle dependence was not clarified.

Electrical properties of trench MOSFETs on various off-angle substances have studied in this study.

$\{11\bar{2}0\}$ or $\{\bar{1}2\bar{1}0\}$ faces tilted by 15° toward $[000\bar{1}]$ bring SiC trench MOSFETs with high channel mobility (~100 cm²/Vs).

2. Fabrication of Trench MOSFET

4°, 8°, 15°–off toward $[\bar{1}\bar{1}20]$ and 8°–off toward $[1\bar{1}00]$
C-face, 4H-SiC, n-Substrates (p-epi)

- Ion implantation (Al, P)
- Trench etching (ICP-RIE (SF_6,Ar,O_2))
- Thermal oxidation (in wet O_2 (1100℃,1.5h) + NO anneal (1150℃,1h))
- Formation of source (Al/Ti) and drain contacts (Ni)
- Metallization annealing (in N_2+H_2 (1000℃,2min))
- Deposition of gate electrodes (Al)

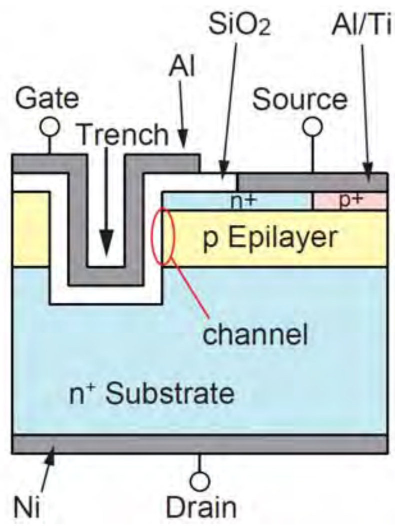

3. Channel Mobility in MOSFET Performance

- The substrate of 15° off-toward $[\bar{1}\bar{1}20]$ shows quite high drain current and high field-effect mobility.

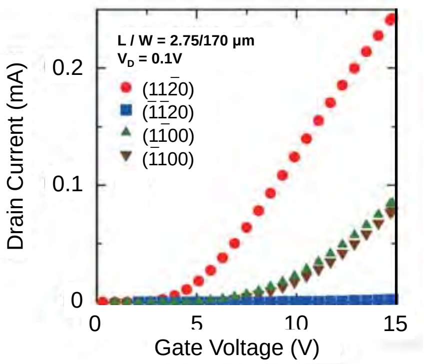

Id-Vg for each plane on 15 off-substrates

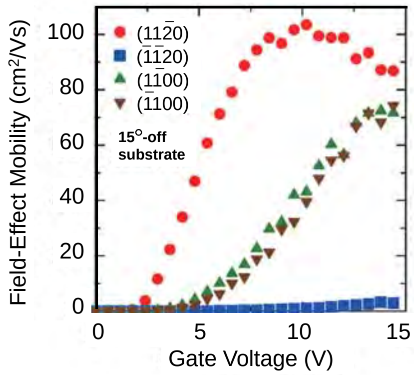

Off angle/Off direction	$(11\bar{2}0)$	$(\bar{1}\bar{1}20)$	$(1\bar{1}00)$	$(\bar{1}100)$
4°/ $[\bar{1}\bar{1}20]$	80	18	60	58
8°/ $[\bar{1}\bar{1}20]$	60	30	56	54
15°/ $[\bar{1}\bar{1}20]$	103	4	72	74
8°/ [1120]	49	46	14	68

Field effect channel mobility for each plane on 15 off-substrates

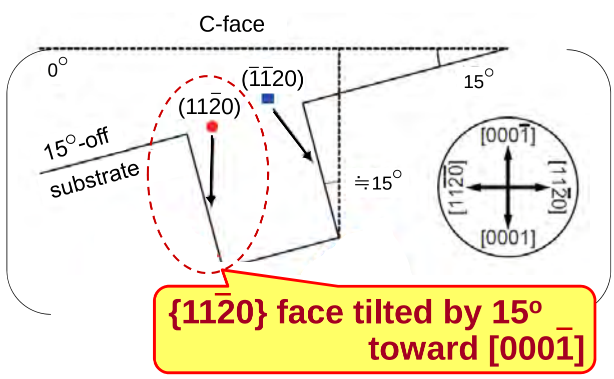

4. Patent available for licensing

Patent No. : WO2012/026089 (JP,US,EP,KR,CN)

Contact : Masaru OZAKI (JST)
phone: +81-3-5214-8486
e-mail: license@jst.go.jp

Advanced Materials

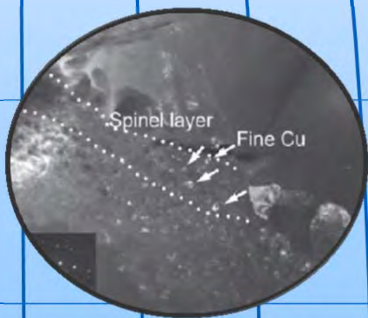

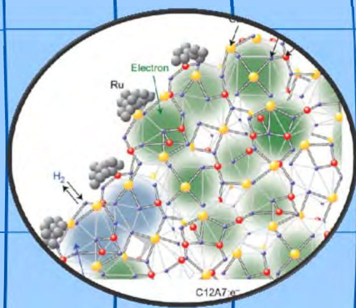

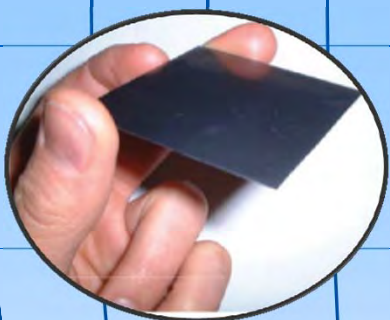

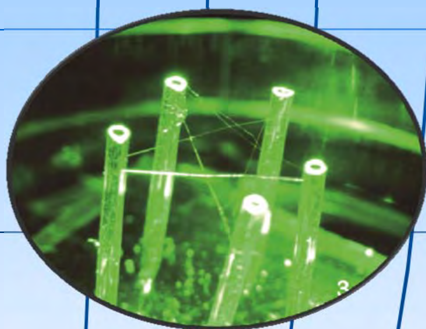

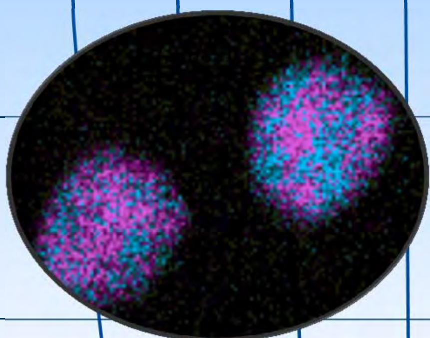

Electro-conductive & Transparent Nano-porous Compound C12A7

Prof. Hideo HOSONO (Tokyo Institute of Technology)

1. Novel Compound $12CaO \cdot 7Al_2O_3$ (i.e.C12A7)

- C12A7 is composed of materials of alumina cements, and has 6 cages with an inner free space of 0.4nm of which only two cages are filled with O^{2-}. These 80% cages are free spaces.
- The oxide ions can be replaced by various anions such as O^-, H^-, OH^-, e^- etc. showing an interesting function for a variety of potential applications.

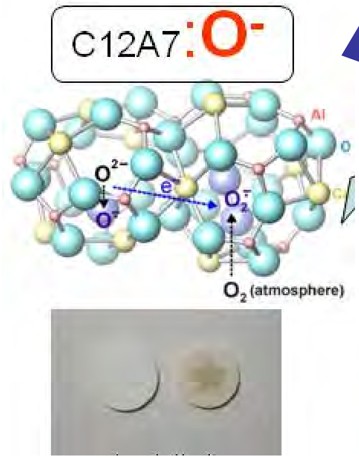

・Strong oxidizer

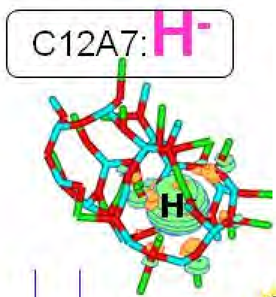

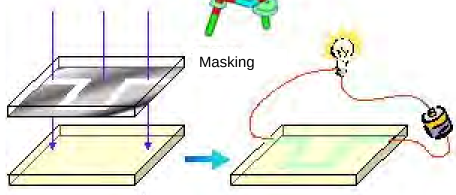

・Electro-conductive by photo-irradiation
・Reducer

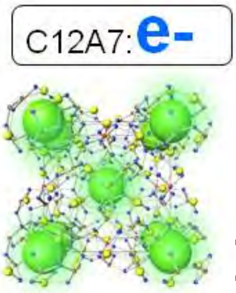

・Highly electro-conductive
・Strong reducer

2. Electride C12A7: e^-

- Conductivity of C12A7: e^-

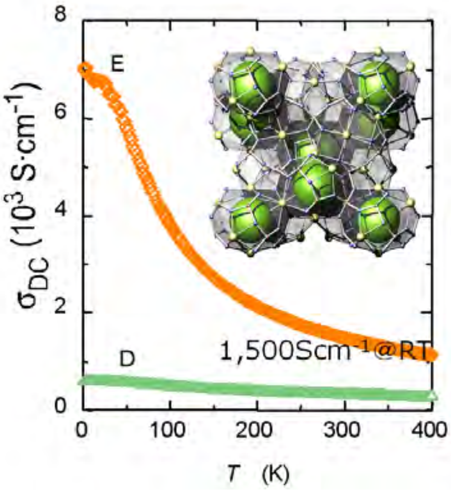

- Cathode ray emission from C12A7: e^-

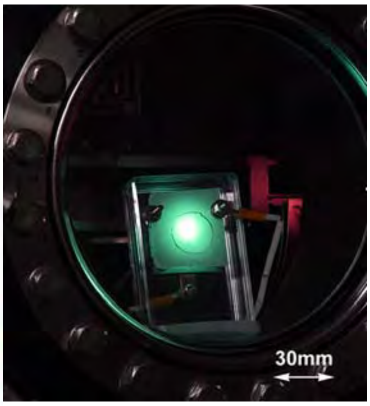

- Reduction reaction using C12A7: e^-

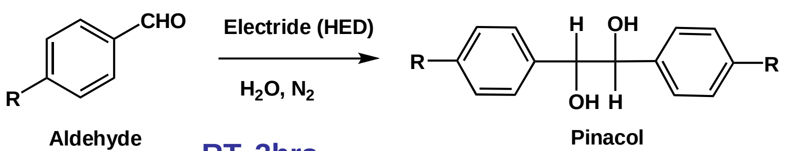

RT, 3hrs

η= 96%

3. Small work function of C12A7: e^-

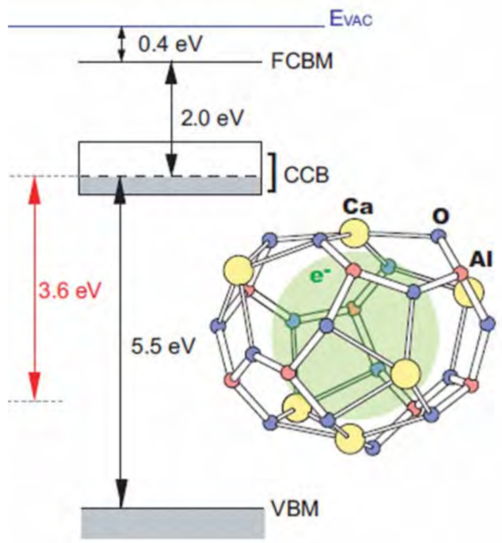

4. Patent available for licensing

Patent No. :US6818192,7462334.7235225,
7507289,7465433,
EP1717217,
JP4147324,4219821,4245608,
TW283234 etc

Contact : Masaru OZAKI (JST)
phone: +81-3-5214-8486
e-mail: license@jst.go.jp

NH_3 Synthesis using a Stable Electride C12A7 as Electron Donor and Reversible Hydrogen Store

Prof. Hideo HOSONO & Prof. Michikazu HARA (Tokyo Institute of Technology)

1. Present Industrial NH_3 Synthesis

- 160 million tons of NH_3 are produced each year through industrial processes at high temperature and high pressure.
- Iron based catalysts (Haber-Bosch method) or Ru metal particles dispersed on a support material in the industrial processes are used.

Haber-Bosch method; $N_2 + H_2 \xrightarrow{Fe} NH_3$

400-600 ℃, 20- 40 MPa

- The determining step is the **dissociation of both N_2 and H_2** on the metallic catalyst surface, and it is also important for the surface not to become covered by H_2 blocking active sites for N_2 dissociation (**→H_2 poisoning**).
- These processes consume a great deal of energy (around 1-2% of worldwide energy apply).

→ **A novel supported Ru catalyst promotes N_2 & H_2 dissociation but suppresses H_2 poisoning**, which will bring big energy savings.

2. Catalytic Performance of Ru-loaded C12A7 Electride for NH_3 Synthesis

- Ru-loaded C12A7;e catalyst activity (TOF) shows one order magnitude greater than some current Ru catalysts. And also the catalyst exhibits the smallest activation energy.

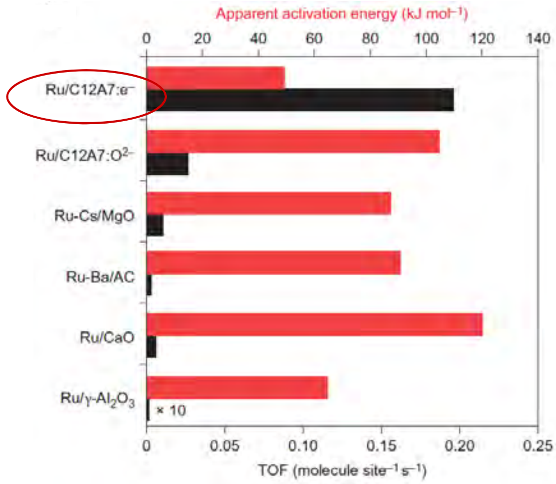

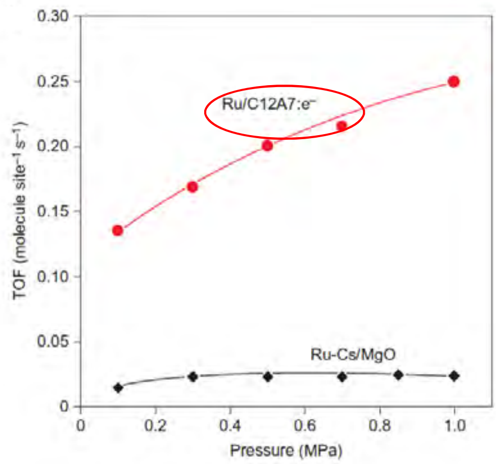

3. Schematic Model of Ru-loaded C12A7 Electride in NH_3 Synthesis

- N≡N bond becomes weakened by electron donating from C12A7;e to the N_2 anti-bonding orbital.
- The C12A7;e also has the role of H_2 scavenger, and transforms H atom to hydride which is reversibly incorporated into the C12A7 nanocages.

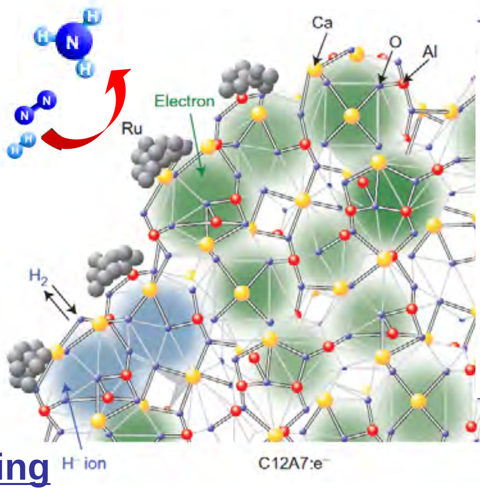

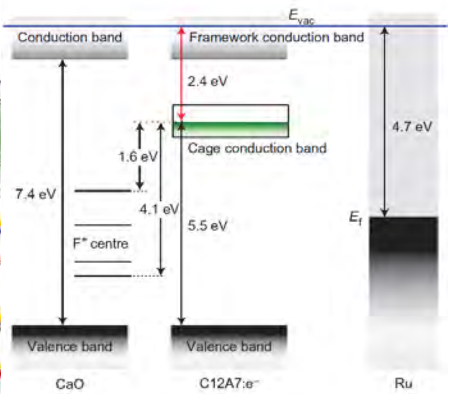

Comparison of energy levels

4. Patent available for licensing

Patent No. : WO/2012/077658

Contact : Masaru OZAKI (JST)
phone: +81-3-5214-8486
e-mail: license@jst.go.jp

Newly developed H_2 Generator using Highly-Oxygen-Permeable Ceria-based Membrane

Prof. Hiroshi TAKAMURA (Tohoku Univ.)

1. Advantages of MPOX (Partial Oxidation of Methane by using Oxygen Permeable Membranes)

- **Objective : Hydrogen generation from natural gas**
- **Comparison of candidate reaction**

	Reaction Formula	ΔG^0_{298} (kJ/mol)	ΔH^0_{298} (kJ/mol)	ΔS^0_{298} (kJ/mol)	drawbacks
Steam reforming	$CH_4 + H_2O \rightarrow CO + 3H_2$	150.843	250.176 (endothermic)	333.164	Slow Start-Ups: Approx. 1h
Partial oxidation	$CH_4 + 1/2O_2 \rightarrow CO + 2H_2$	-86.347	−35.654 (exothermic)	170.024	Large Exergy Loss

- **Partial Oxidation of Methane (POX)**
  Can Large Exergy loss (EXL) of POX be reduced?

Exergy Analysis
Combination with the reaction with exergy vector having opposite direction to POX is promising.

- **MPOX : Membrane separation process + POX ($\Delta G > 0, \Delta S < 0$)**
- **Reduction of EXL of POX is achieved.**

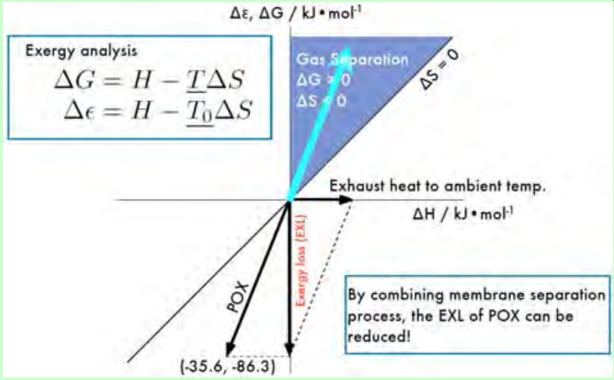

Exergy Analysis shows the advantage of MPOX (POX+ Gas Separation)

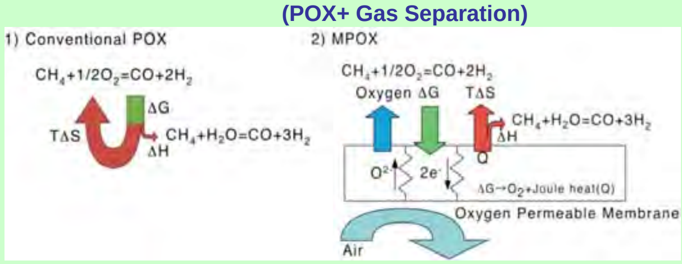

MPOX effectively utilizes the free energy generated from partial oxidation reaction to Oxygen separation

2. Ceria-based oxygen permeable membranes

	Composition	Oxygen flux density μmol • cm^{-2} • s^{-1}	Temp. °C	Ref.
BSCF	$Ba_{0.5}Sr_{0.5}Co_{0.8}Fe_{0.2}O_3$	8.6	875	Shao *et al.*, 2001
LSGF	$La_{0.7}Sr_{0.3}Ga_{0.6}Fe_{0.4}O_3$	8.2	1000	Ishihara *et al.*, 2002
PSAF	$Pr_{0.7}Sr_{0.3}Fe_{0.8}Al_{0.2}O_3$	8.2	1000	Takamura *et al.*, 2002
Ceria-MFO	$(Ce, Sm)O_2$-15vol%$MnFe_2O_4$	10.0	1000	Takamura *et al.*, 2002
LBSFI	$(La_{0.5}Ba_{0.3}Sr_{0.2})(Fe_{0.6}In_{0.4})O_3$	10.6	1000	Aizumi *et al.*, 2004

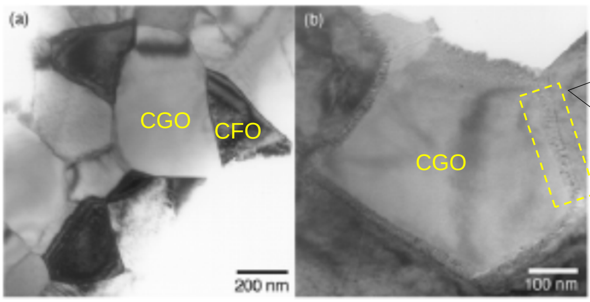

Grain boundary
- nano-sized CGO
- spinel-type ferrite grains.

Ceria-MFO : $(Ce,Gd)O_2$-17vol%$CoFe_2O_4$ fired at 1300℃ for 2 h

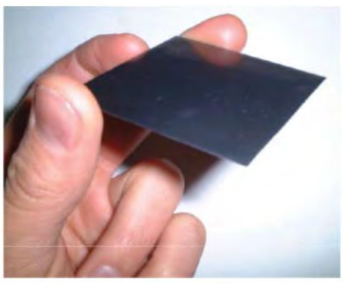

CSO membrane made by tape-casting tequnique: 5cm × 5cm

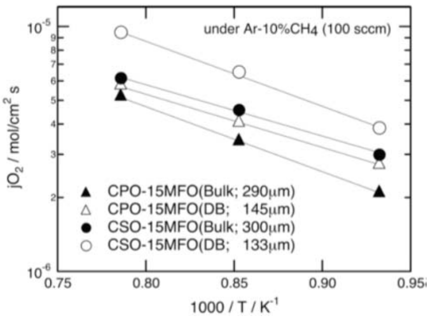

Oxygen permeation properties

Ceria-MFO: $(Ce,Re)O_2$ + $MeFe_2O_4$
- $(Ce,Re)O_2$: Oxygen Conductive Phase (Re is an acceptor) (CGO (Re=Gd), CSO (Re=Sm) and CPO (Re=Pr))
- $MeFe_2O_4$: Electron Conductive Phase

3. Characteristics of MPOX reformer

No. of modules	CH_4 (sccm)	Air (sccm)	Temp. (℃)	S/C	jO_2 (μmol/cm^2 s)	CH_4 conv. (%)	CO selectivity (%)	H_2 selectivity (%)
1	150	500	780	0.88	3.3	96	84	89

※C-balance: 150 sccm (input); 151.8 sccm (output)

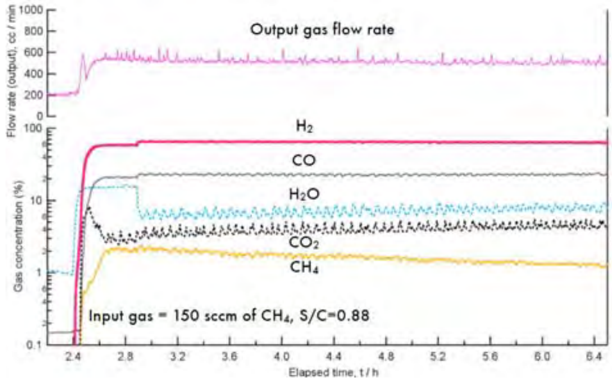

Flow rate and composition of reformate gas

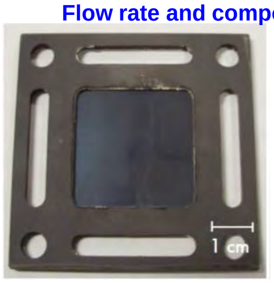

MPOX reformer module comprising of CSO.15MFO and ZMG232R (left) and its 20 stacks (right)

To produce 10 liter/min of hydrogen, stack of 20 modules is required.

4. Patent available for licensing

Patent No. : WO/2003/084894,WO/2007/046314 (JP,US,EP)

Contact : Takuji OHINATA (JST)
phone: +81-3-5214-8486, e-mail: license@jst.go.jp

PdRu Solid-Solution Alloy Nanoparticles with Enhanced CO Oxidization Activity

Prof. Hiroshi KITAGAWA (Kyoto University)

1. Solid-Solution Alloy

- Mixed metal at the atomic level
- Have the advantage of easily controlling chemical and physical properties by changing compositions and/or combinations

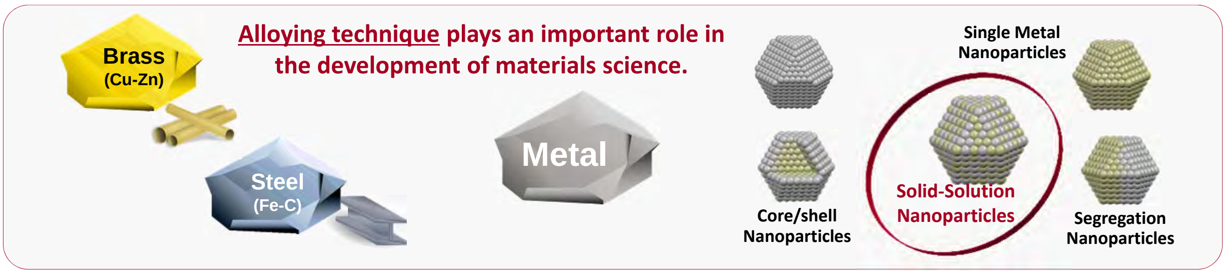

However・・・

Solid-solution phases are limited by combinations, compositions and/or temperature.

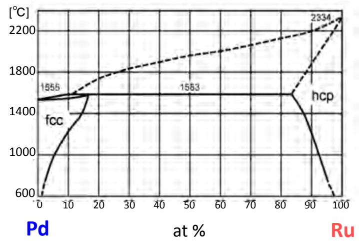

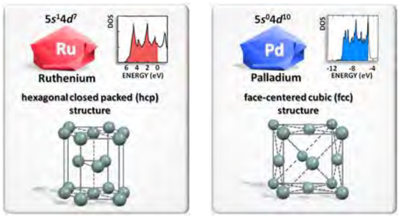

PdRu solid-solution alloys had not yet obtained….

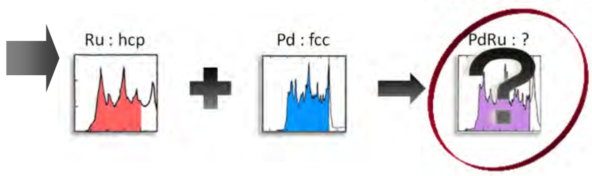

2. NOVEL Synthesis Process

Triethyleneglycol (Reducing agent) + PVP (Protecting agent)
poly(*N*-vinyl-2-pyrrolidone

Pd^{2+}+ Ru^{3+} aqueous solution

[Pd : Ru = x : 1-x
(x = 0, 0.1, 0.3, 0.5, 0.7, 0.9, 0.95, 1)]

Pd_xRu_{1-x} nanoparticles

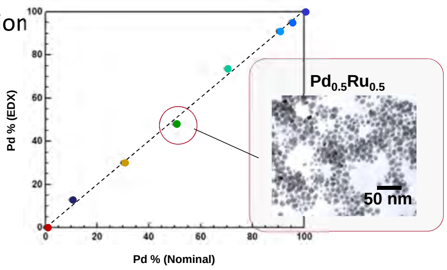

- Elemental Mapping Images of $Pd_{0.5}Ru_{0.5}$ NPs

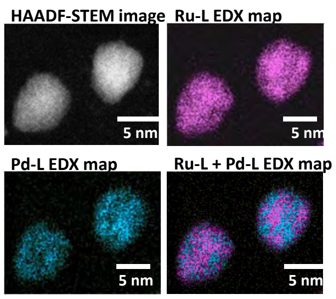

- Compositional Line Profiles

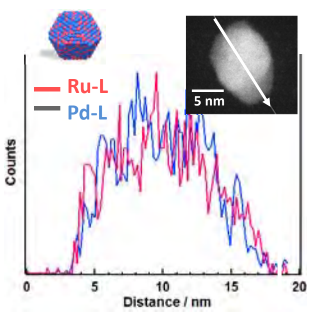

- Powder X-ray Diffraction (XRD) Patterns

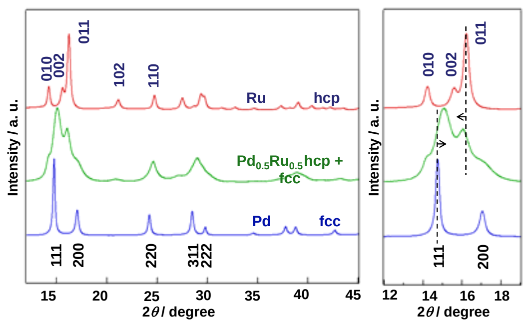

3. CO Oxidation Catalyst

- The **Pd-Ru solid-solution alloy** oxidizes carbon monoxide at much lower temperature..

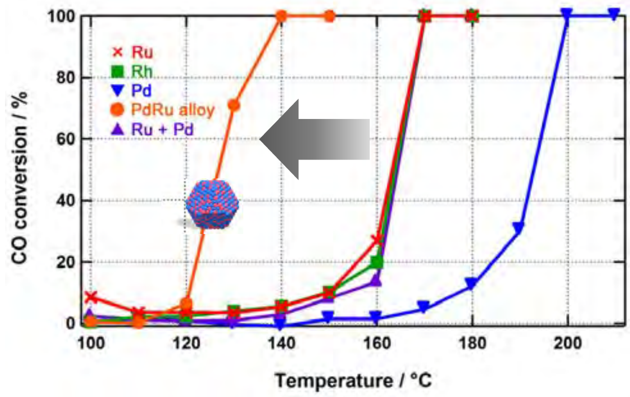

Condition: Catalyst : $Al_2O_3(\gamma)$-supported Pd-Ru NPs
Reaction Gas : $He/CO/O_2$

The Pd-Ru solid-solution alloy performs significantly higher activity than any of other metal nanoparticles in single phase, so it is expected to serve as a high-performance catalyst surpassing the conventional catalysts.

4. Patent available for licensing

Patent No. : JP2012-204292
(International application is in preparation.)

Contact : Miho OKISHIRO (JST)
phone:+81-3-5214-8486
e-mail: license@jst.go.jp

Ru Nanoparticles with fcc Structure for High-activity Catalyst

Prof. Hiroshi KITAGAWA (Kyoto University)

1. Ruthenium Nanoparticles

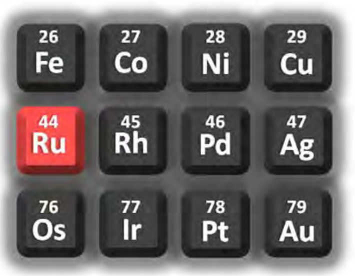

Ruthenium is extensively used as catalyst:

- Organic synthesis
- CO removal from car exhaust or fuel–cell systems

However,
<u>the conventional synthesis process results in merely the hcp-Ru, meaning that there was no convenient way able to produce fcc-Ru nanoparticles.</u>

Application example "ENE･FARM" : Ru catalyst is used within the household fuel-cell cogeneration system.

hcp $5s^1 4d^7$

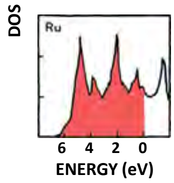

This study successfully meet the demand for synthesizing fcc-Ru nanoparticles, serving as high-active catalyst.

fcc : face-centered cubic
hcp : hexagonal closed packed structure

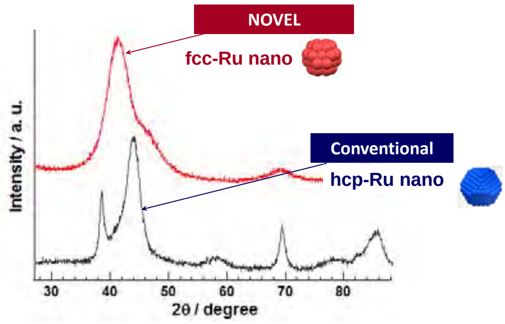

2. NOVEL Synthesis Process

- Substantial fcc-Ru nanoparticles
- Single-step synthesis
- Particle size controllable

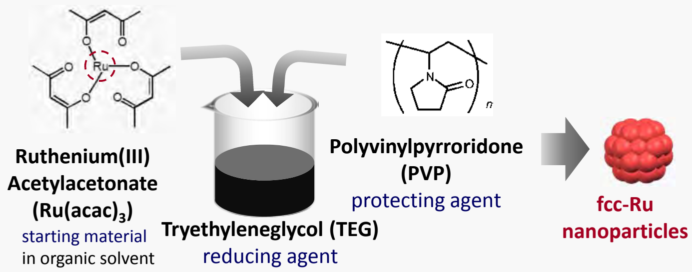

Particle size is controllable by varying the synthesis condition.

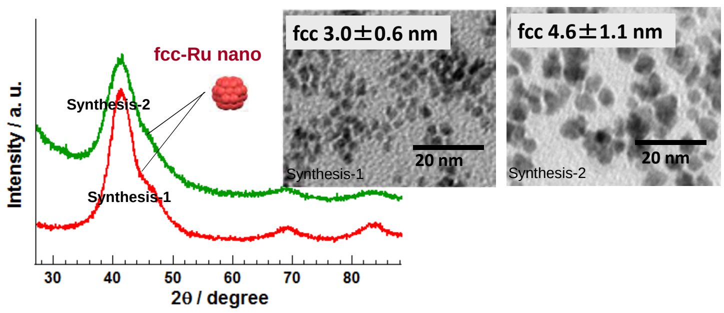

XRD patterns

3. CO Oxidation Catalyst

- The fcc-Ru catalyst oxidizes carbon monoxide at lower temperature than hcp-Ru catalyst.

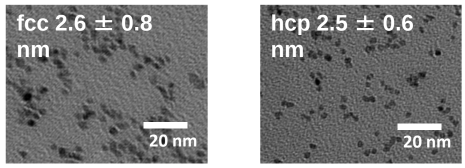

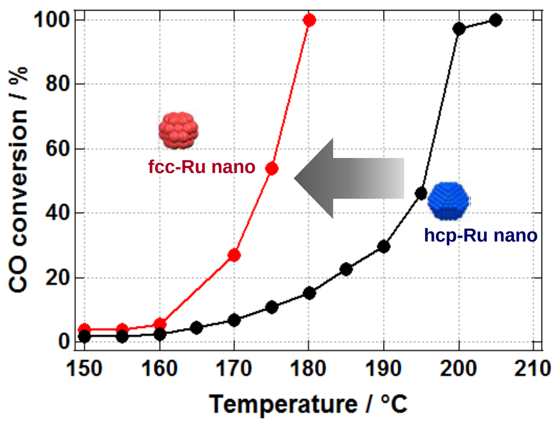

Condition: Catalyst Quantity : 0.075 g, $Al_2O_3(\gamma)$-supported Ru
Reaction Gas : $He/CO/O_2$ = 49/0.5/0.5 (cc/min)
Reaction temperature : 150 ℃～

The fcc-Ru catalyst, firstly prepared by the novel synthesis process, performs significantly higher activity than the hcp-Ru catalyst.

4. Patent available for licensing

Patent No. : PCT/JP2012/005838 (JP, US)

Contact : Miho OKISHIRO (JST)
phone:+81-3-5214-8486
e-mail: license@jst.go.jp

Application of Leached Al-Cu-Fe Quasicrystal to Steam Reforming of Methanol

Prof. An-Pang TSAI (Tohoku University)

1. Motivation to Catalytic Application of QC

- So far, research on quasicrystals (QCs) has been purely academic.
- What is found as general physical properties of QCs are:

1) Themodynamically stable
2) Stable up to high temperature
3) Very brittle ･･･ easy to obtain powder form by crushing
4) High-specific surface area
5) Extreme high resistivity : a few thousand of μΩcm
6) Hardness comparable to silica : 800～1000Hv
7) Low friction coefficient comparable to Diamond

Application to Catalyst is promising.

Candidate Materials:

$Al_{63}Cu_{25}Fe_{12}$

- Al, Cu, Fe : abundant and cheap
- Cu : various catalytic behavior

2. Catalyst preparation to SRM reaction

(1) Precursor Quasicrystal Preparation

Al-Cu-Fe QC alloy ingots (prepared in Argon atmosphere in arc furnace)

↓ Annealing: 24h at 800℃

↓ Crushing and Screening

↓ **Precursor Quasicrystal with size 20～ 53μm**

(2) Catalyst Preparation

↓ Alkali leaching by 5wt% NaOH aqueous solution for 4h room temperature to remove Al

↓ Filtered out and washed with distilled water

↓ Dried at 50℃ overnight

↓ **Leached Powder（before Calcination）････ (a)**

↓ Calcined at 600℃ for 3h in air

↓ **Calcined QC powder ････ (b)**

(3) SRM reaction

($CH_4OH + H_2O \rightarrow 3H_2 + CO_2$)

↓ Activation in H_2 atmosphere at 200～300℃

$Cu_xFe_{3-x-y}Al_yO_4 \rightarrow Cu + (Fe,Al)_3O_4$
$CuO \rightarrow Cu$ ····· (c)

↓ Steam Reforming Reaction（SRM）

(Reduction of Catalyst by H_2 generated from SRM reaction occurs)

3. Structural Changes: TEM image

(a) Before Calcination

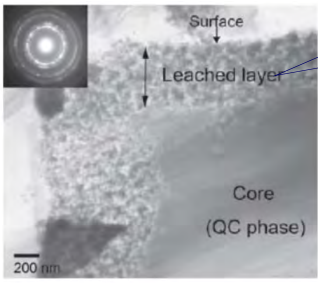

Homogenous mixture of oxides containing Cu, Fe, Al

- BFI of cross-section of QC *before Calcination* (Insert electron pattern obtained from the leached layer)

(b) After Calcination

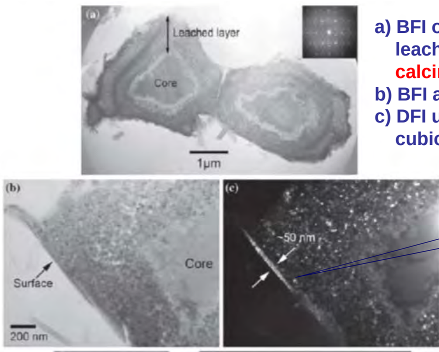

a) BFI of cross-section of NaOH leached Al–Cu–Fe QC alloy after calcination at 600℃
b) BFI around the leached layer
c) DFI using 2–20 reflection of cubic spinel at the surface,

Spinel Layer: $Cu_xFe_{3-x-y}AlyO_4$

(c) After Calcination followed by H_2 reduction

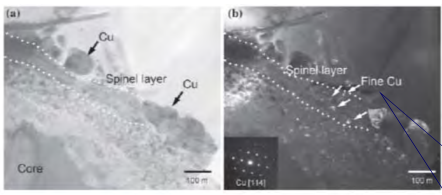

a) BFI of leached area of NaOH-leached Al–Cu–Fe QC alloy after calcination at 600℃ followed by H_2 reduction at 300℃
b) DFI using 2–20 reflection of Cu.

Fine Cu: key factor for catalytic activity enhancement

4. Physical Properties and Catalytic Activities

Catalyst	Cu crystallite size[b] (nm)	BET surface area (m^2/g_{-cat})	N_2O titration[d] (μmol/g_{-cat})	H_2 production rate[e] per catalyst weight (μmol/s/g_{-cat})	H_2 production rate[e] per surface area (μmol/s/m^2_{cat})	H_2 production rate[e] per N_2O titration (μmol/s/μmol(N_2O))	CO selectivity[e] (%)	
Leached QC	21	20.0	116.8	306.9	15.3	2.63	1.3	(b)
Leached QC with calcination	31 (10)[c]	5.0	126.6	405.0	81.0	3.20	1.2	(c)
Cu/ZnO[a]	10	57.3	262.2	372.2	6.5	1.42	1.5	
CuO	66	2.4	12.2	15.4 : small	6.4	1.26	-	
$CuFeAlO_4$	13	1.7	67.7	242.2 : large	142.4	3.58	1.2	

- Cu/ZnO : commercial SRM catalyst
- Both CuO and $CuFeAlO_4$ reside in calcined QC.

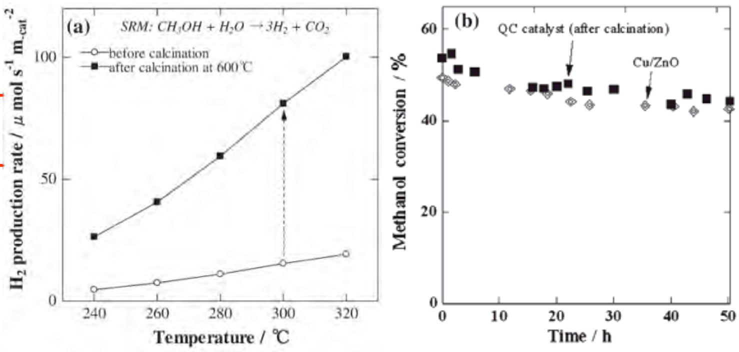

5. Patent available for licensing

Patent No. : 7592292(US), 284059(TW) (EP, JP (under examination))

Contact : Takuji OHINATA (JST)
phone: +81-3-5214-8486, e-mail: license@jst.go.jp

Abbreviations
BFI : Bright Field Image of TEM
DFI : Dark Field Image of TEM
SAD : Selected Area Electron Diffraction
SRM : Steam Reforming of Methanol

Two Types of Ferrous Polycrystalline Shape-Memory Alloys Showing Superelasticity (FeNiCoAlTaB, FeMnAlNi)

Prof. Ryosuke KAINUMA,
Asst. Prof. Toshihiro OMORI (Tohoku University)

1. The Ways to Give Superelasticity to SMAs

- **Shape Memory Effect･･･heating is required to return to original state (original shape).**
- **Superelasticity ･･･heating is *not* required to return to original state (elastic deformation).**

⬇

- **Martensitic transformation should be thermoelastic to gain superelasticity.**

⬇

- **Introduction of (partially) ordered phase is required.**

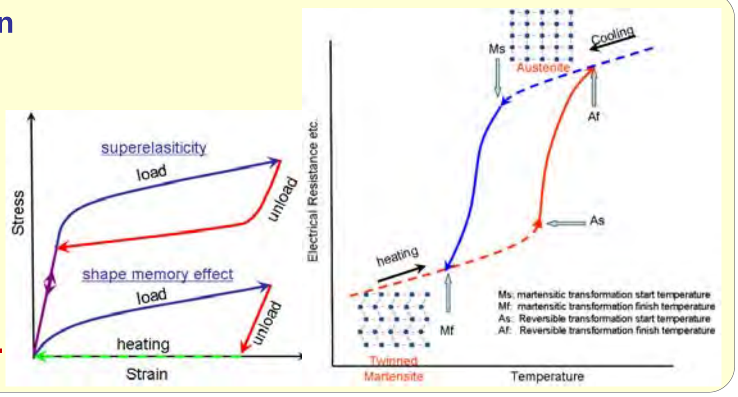

2. Alloy Design of FeNiCoAl and FeMnAl alloys with ordered precipitates

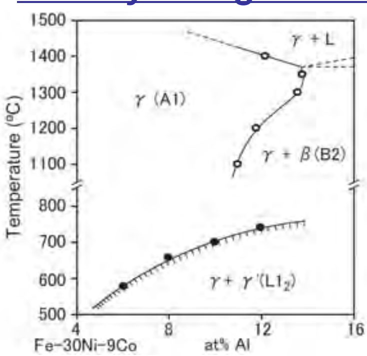

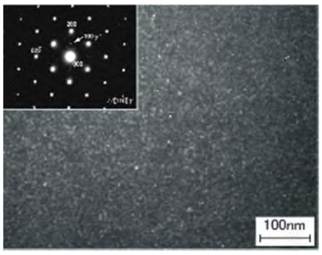

FeNiCoAl:γ'(L12)(ordered phase) precipitates coherently in γ matrix.

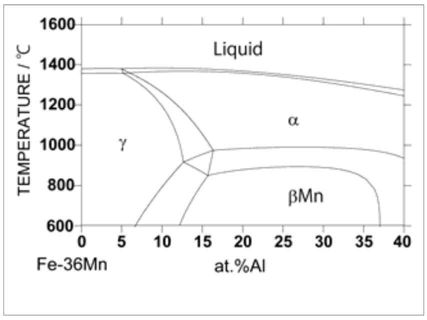

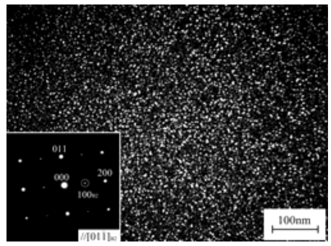

FeMnAlNi:B2(ordered phase) precipitates coherently in A2 matrix.

3. Thermoelasiticity (only for FeNiCoAl)

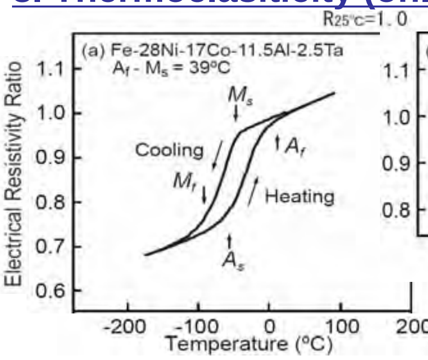

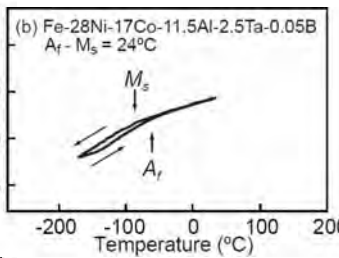

Thermoelastic behavior of FeNiCoAlTa(B)

4. Superelastic Properties

FeNiCoAlTaB

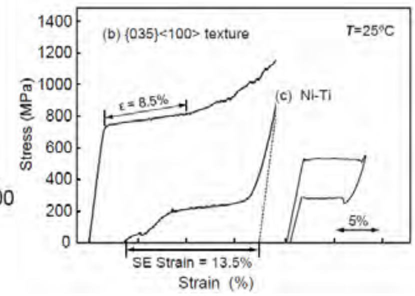

FeMnAlNi

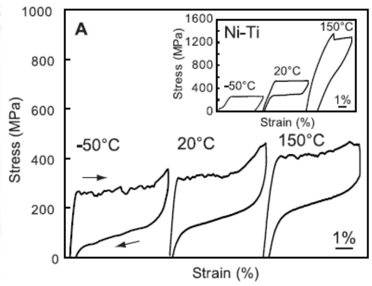

5. Comparison with Conventional Metal Alloys

Alloy system	Crystal structure		Chemical composition (at%)	ΔS (J mol⁻¹K⁻¹)	ε_{SE} (%)	$\frac{d\sigma_c}{dT}$ (MPa °C⁻¹)
	Parent	Martensite				
Fe-Mn-Al-Ni	BCC (A2+B2)	FCC	$Fe_{43.5}Mn_{34}Al_{15}Ni_{7.5}$	-0.43	5.2	0.53
Fe-Ni-Co-Al	FCC	BCT	$Fe_{40.95}Ni_{28}Co_{17}Al_{11.5}Ta_{2.5}B_{0.05}$	-2.95	13.5	3.1
Ti-Ni	B2	B19'	$Ti_{50}Ni_{50}$	-4.37	7.3	5.7
Ti-Ni-Cu	B2	B19	$Ti_{50}Ni_{40}Cu_{10}$	-2.92	3.2	8.4
Cu-Al-Ni	$D0_3$	6M	$Cu_{68.4}Al_{27.8}Ni_{3.8}$	-1.03	8.6†	1.5‡
	$D0_3$	2O		-1.20	4.7†	3.4‡
Cu-Zn-Al	$D0_3$	6M	$Cu_{67.9}Zn_{16.1}Al_{16}$	-1.45	8.5†	2.1‡
Cu-Al-Mn	$L2_1$	6M	$Cu_{71.9}Al_{16.6}Mn_{9.3}Ni_2B_{0.2}$	-1.15	7.5	2.4
Ni-Mn-Ga	$L2_1$	10M	$Ni_{52}Mn_{24.4}Ga_{23.6}$	-0.97	4.0†	3.5‡
Ni-Fe-Ga	$L2_1$	14M	$Ni_{51}Fe_{22}Ga_{27}$	-0.91	6.2†	1.9‡
Ti-Nb	BCC	Orthorhombic	$Ti_{74}Nb_{26}$	-1.30	2.3	4.4

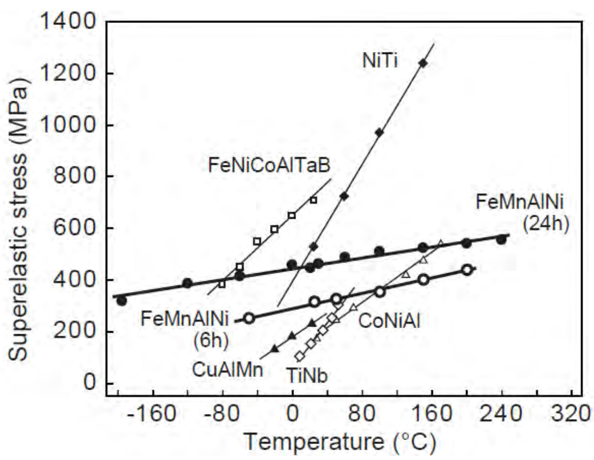

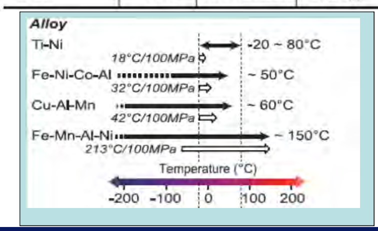

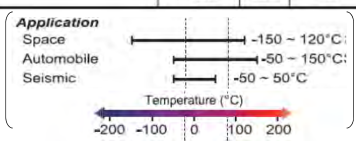

6. Patent available for licensing

Patent No. :WO2007/055155, WO2011/046055 (JP, US, EP, CN, KR, CA)

Contact : Takuji OHINATA (JST)
phone: +81-3-5214-8486
e-mail: license@jst.go.jp

http://www.jst.go.jp/tt/EN/

Cobalt-Based High-Temperature Alloys

Prof. Emeritus Kiyohito ISHIDA,
Asst. Prof.Toshihiro OMORI (Tohoku University)

1. Beyond Ni-based Superalloys

- Co-based alloys' properties as superalloys candidate (compared to Ni-based superalloys)
  1) Higher melting point ･･･favorable
  2) Lower strength ････ ･･･unfavorable

Precipitation hardening of matrix by ordered phase is necessary as in the case of Ni-based superalloys.

- γ+γ' phase in Co-Al-W was discovered

Base Element	Melting Point (K)	Superalloys	Crystal Structure of Superalloys	
Nickel (Ni)	1,728	Ni-Al-Ti	matrix	γ(FCC)
			Ordered phase	γ'(Ni_3(Al,Ti)) with $L1_2$ structure)
Cobalt (Co)	1,768	Co-Al-W (this study)	matrix	γ(FCC)
			Ordered phase	γ'(Co_3(Al,W) with $L1_2$ structure)

Co-Al-W superalloys

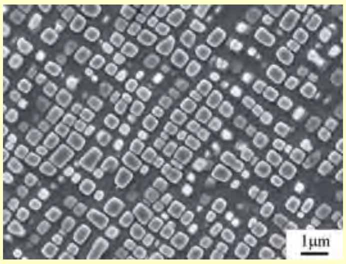

Phase of Newly developed Co-Al-W alloys

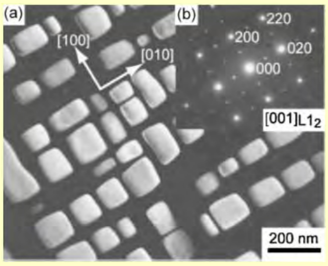

Precipitated phase was confirmed asγ' phase

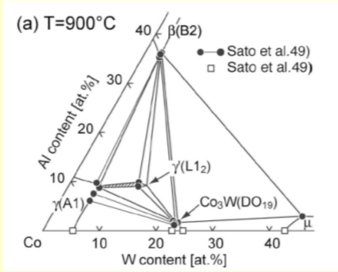

Phase diagrams of the Co-Al-W ternary system

Ni-based superalloys

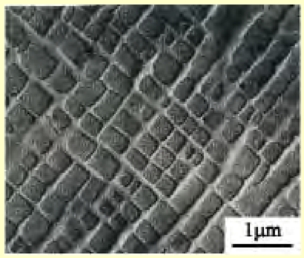

γ+γ' phase in Ni-based superalloys for comparison

2. Properties of New Alloys

(a) DSC curves

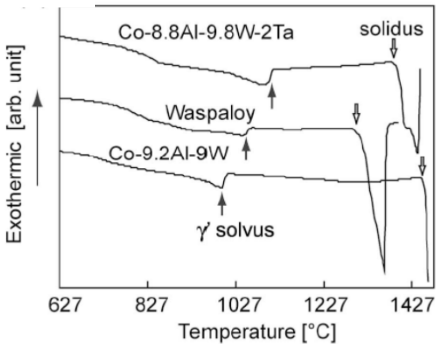

(b) Vickers Hardness of various alloys

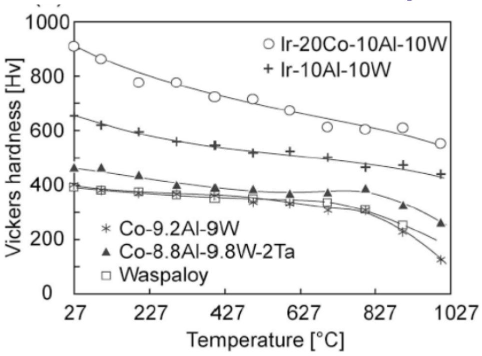

(C)Temperature dependence of 0.2% Flow Stress

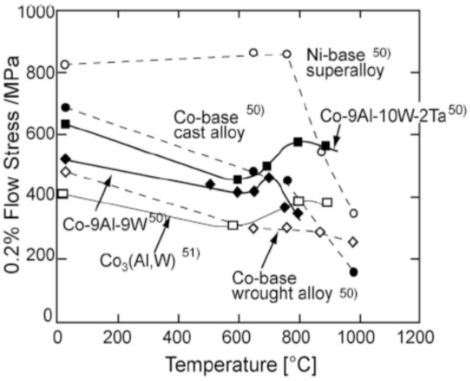

3. Application Examples

(1) High hot-workability

Hot rolling at 1,250℃

(2) Application to a Friction-Stir-Welding tool

Before Welding

After Welding

Welded Sample (Two Ti plates are welded)

4. Patent available for licensing

Patent No. : WO2007/032293, WO2007/091576 (JP,US,EP,CN,CA)

Contact : Takuji OHINATA (JST)
phone: +81-3-5214-8486
e-mail: license@jst.go.jp

Excellent Mechanical Properties of Hybridized Carbon Nano-composite Thin Films

Dr. Eiji IWAMURA (Arakawa Chemical Ind. Ltd.
formerly, University of Tokyo)

1. Fabrication of Hybridized Carbon Films

- **Sputtering method** is used under the conditions of both low temperature of substrate and high pressure of atmosphere gas for fabrication of **network structures consisting of columns and inter-column regions in a-C films.**

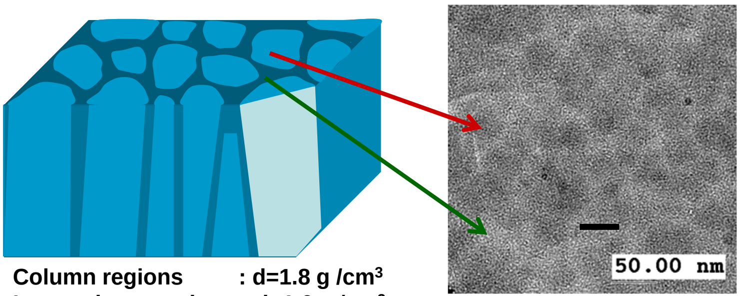

Column regions : d=1.8 g /cm^3
Inter-column regions : d=1.6 g /cm^3

Hybridized a-C film :

- Thickness: 500 nm
- Sputter deposited on Si wafer
- Substrate : Room temp.
- Ar+CH_4 gas pressure: 4Pa

2. Structural Modification by Low-energy EB Irradiation

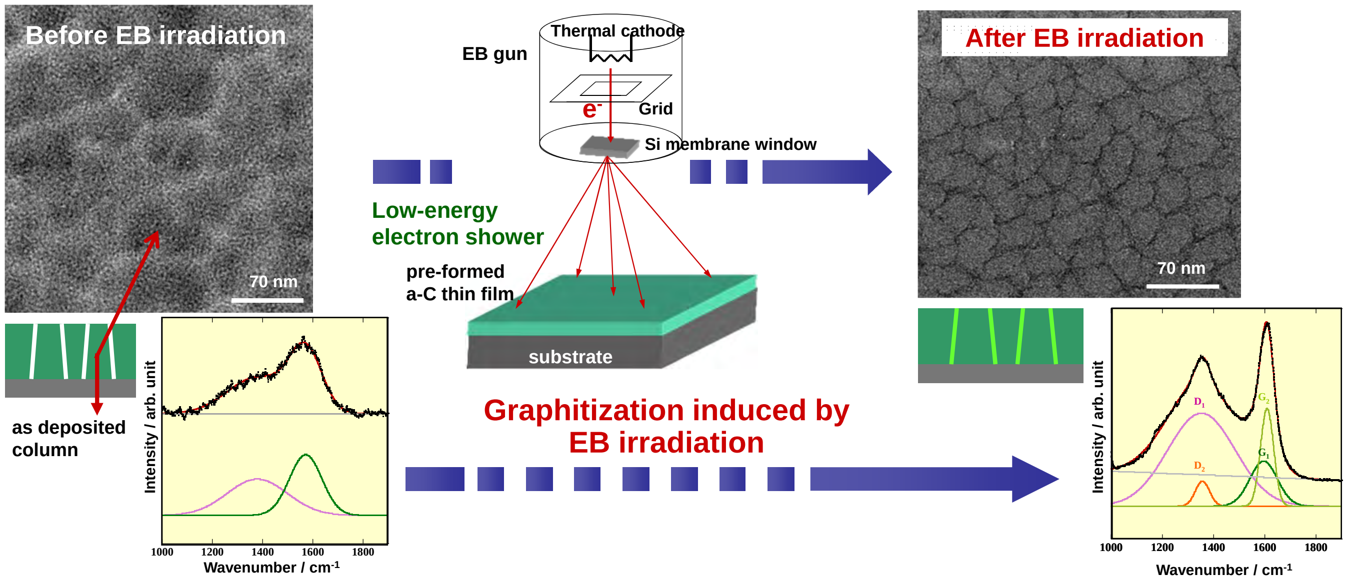

3. Mechanical Properties of EB Irradiated Film

- **EB irradiated film** shows not only **superior wear resistance** but also **high elasticity.**

Film Hardness : Nanoindentation Test

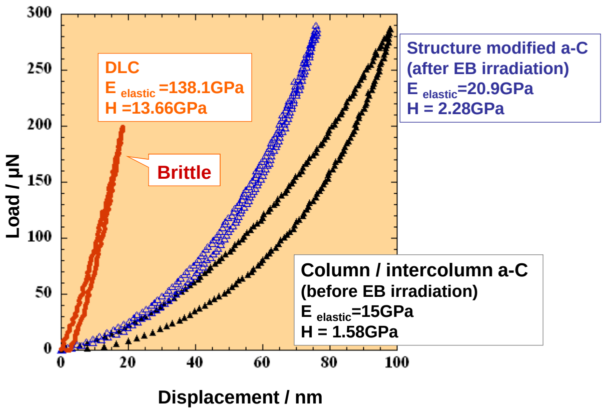

Micro-wear Resistance Test

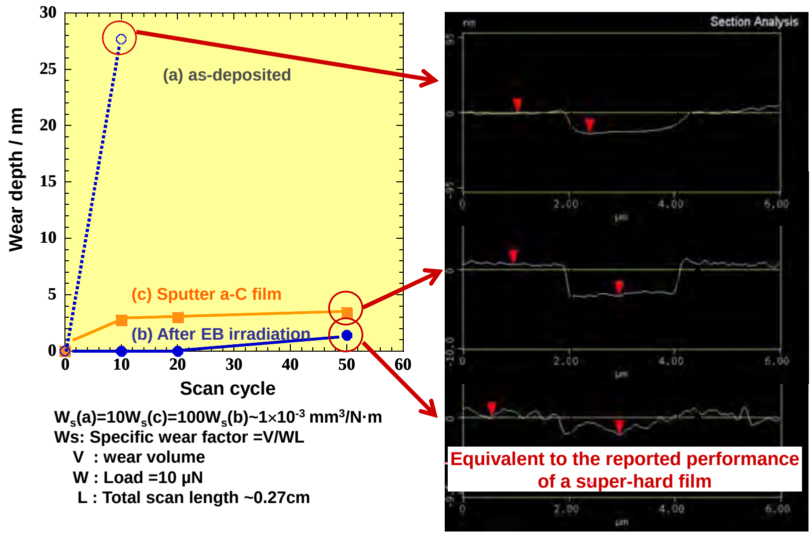

$W_s(a)=10W_s(c)=100W_s(b)\sim 1\times 10^{-3}$ mm^3/N·m
Ws: Specific wear factor =V/WL
V : wear volume
W : Load =10 μN
L : Total scan length ~0.27cm

4. Patent available for licensing

Patent No. : WO/2005/083144

Contact : Masaru OZAKI (JST)
phone: +81-3-5214-8486
e-mail: license@jst.go.jp

Hydrogen Storage Material using Hybridized Carbon Nano-composite

Dr. Eiji IWAMURA (Arakawa Chemical Ind. Ltd.
formerly, University of Tokyo)

1. Fabrication of Hybridized Carbon Films including Metal (ex. Ti, Y, Zr, Hf)

●**Sputtering method** with two target materials (graphite and metal) is used.
●**Metals are located in the column regions** in network carbon structures (columns and inter-column regions) of a-C films.

Fabrication condition of hybridized a-C film including metal

- Targets : Graphite and metal (e.g. Ti , Y, Zr, Hf)
- Sputter deposited on Si wafer
- Substrate temp. : Room temp.
- Ar gas pressure : 2 Pa
- Thickness : 2μm

Hybridized a-C film including Ti metal
(White color part is Ti metal.)

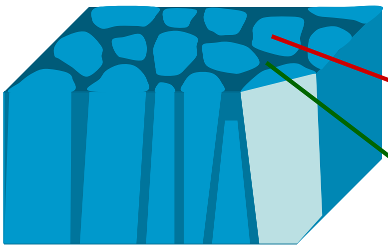

Column regions : d =1.8 g/cm³
Inter-column regions : d =1.6 g/cm³

Hybridized a-C film

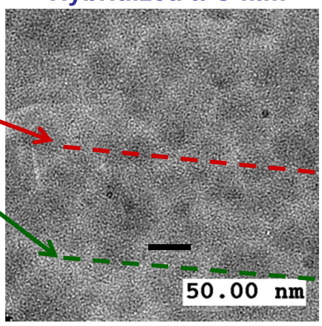

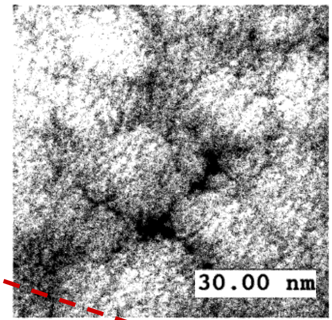

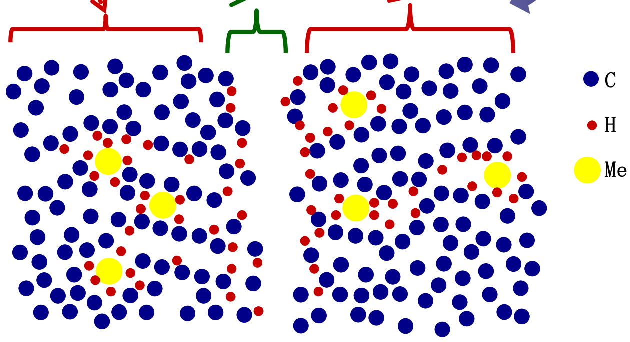

- ● Ti metals are located in column regions of hybridized a-C film.
- ● Hydrogen is almost stored on the surface of metals within the columns.
- ● Hydrogen is repeatedly stored and released through inter-column regions. The release temperature is low (~600K).

2. Characteristic Table of Storing / Releasing Hydrogen

Metal	w%	Substrate Temp. (K)	Ar pressure (Pa)	Release Temp. (K)	H_2 stored initial volume (atm%)	H_2 stored volume after 5 cycles (atm%)
None	0	283	1.99983	600	2.0	5.0
Ti	12.5	283	1.99983	600	14.0	13.0
Y	3.0	283	1.99983	600	16.0	16.0
Zr	8.0	283	1.99983	600	13.6	13.2
Hf	26.0	283	1.99983	600	12.5	10.8

3. Patent available for licensing

Patent No. : WO/2004/067166
(JP,US,EP,KR,CN)
Contact : Masaru OZAKI (JST)
phone: +81-3-5214-8486
e-mail: license@jst.go.jp

Template Synthesis in Hydrodynamically-Aligned Supramolecular Nano-channels

Dr. Daisuke KIRIYA, Dr.Hiroaki ONOE, et.al (Takeuchi Lab, University of Tokyo)

1. Hydrodynamically-Aligned Supramolecular Nano-channels

- Supramolecular assembly has been essential from material science to biological science.
- **Nanochannel** is expected as a nano-scale reaction vessel.

Two problems to solve

1. Entanglement of supramolecular nanofibers
   ➡ Need to prevent entanglement by using "Microfluidics"
2. Poor handle-ability because of low mechanical strength
   ➡ Need to increase mechanical strength by encapsulation in a robust polymer

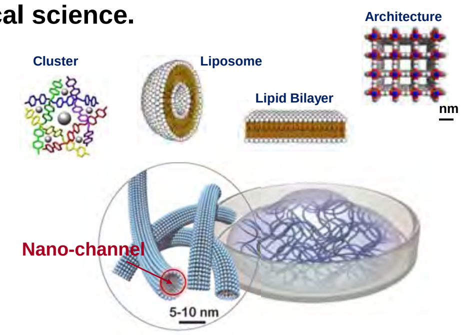

2. Synthetic Process

- Linearly-aligned Jacketed supramolecular fibers are fabricated in a coaxial flow microfluidic device.

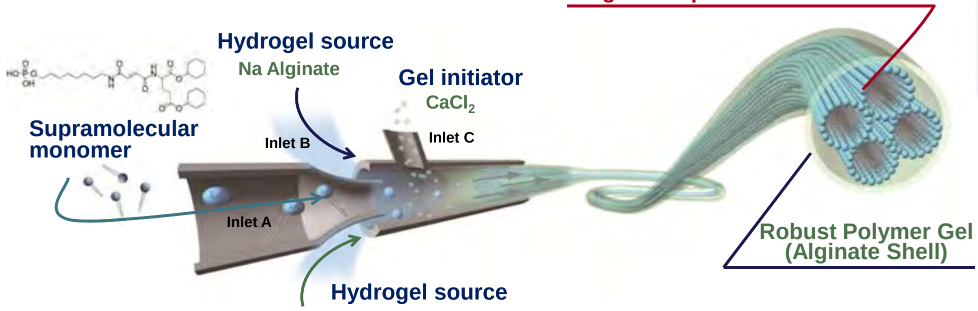

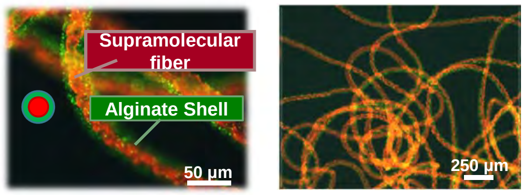

Supramolecular monomers are self-assembled monomers along one direction

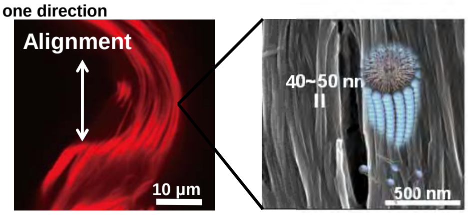

3. Handling of Supramolecular Nanofibers

- Appropriate features for practical applications
  1. Aligned supramolecular nanofibers
  2. Easy-to-handle core-shell nanofibers

- **Meter-long core-shell fiber**

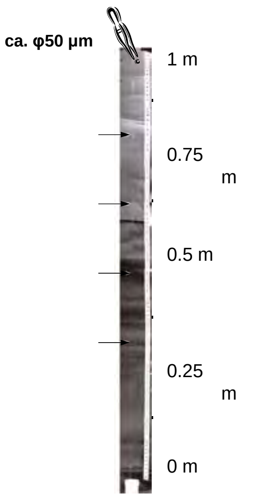

- **Sufficient strength**

A single jacketed supramolecular nanofiber bridging five glass pillars to form a star shape in air

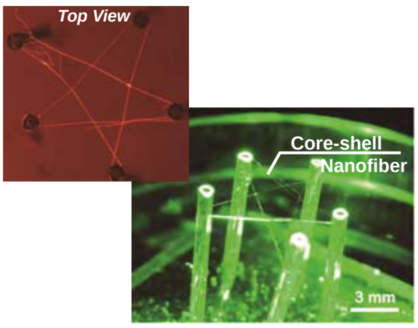

Potential applications
Scaffold for cell culture, Nano-scale reaction vessel

4. Synthesis as Reaction Vessels

- Template Synthesis in Hydrophobic Nano-Channels

PEDOT is extensively applied as a conductive polymer, however, its insolubility makes pure PEDOT difficult to handle.

PEDOT Poly(3,4-ethylenedioxythiophene)

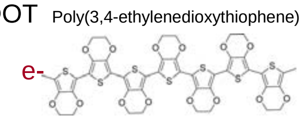

Potential applications
Biochemical molecules, proteins, nano-particles, metals for generating large oriented materials, etc.

- **Polymerization of PEDOTs**

The process involves a step of causing supramolecular monomers to self-assemble in a micro channel.

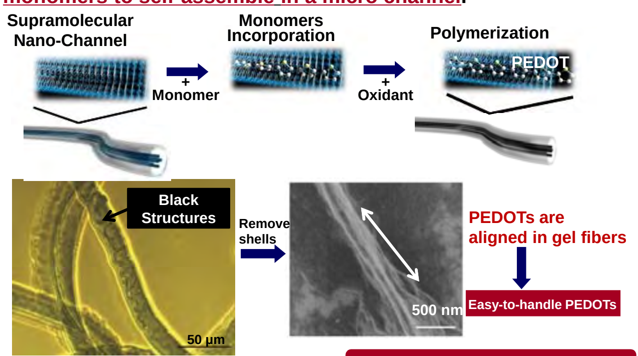

- **Example Application**

PEDOTs incorporated in microfluidic channel

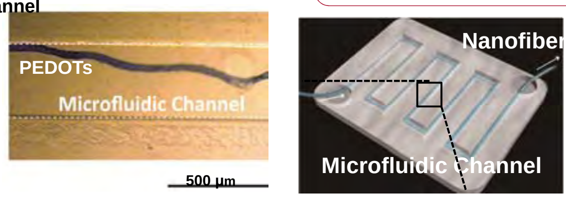

Potential applications
Flexible organic circuits, Sensors

5. Patent available for licensing

Patent No. : WO/2011/089753 (US, JP)

Contact : Miho OKISHIRO (JST)
phone:+81-3-5214-8486
e-mail: license@jst.go.jp

Measurement Equipment

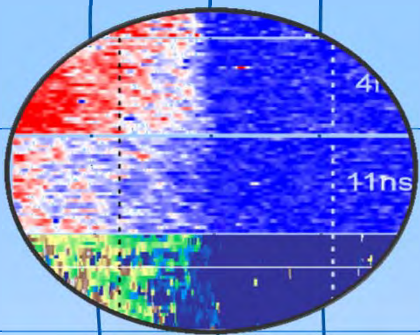

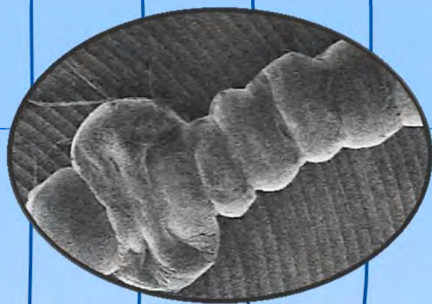

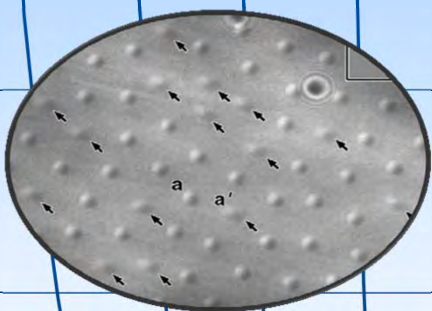

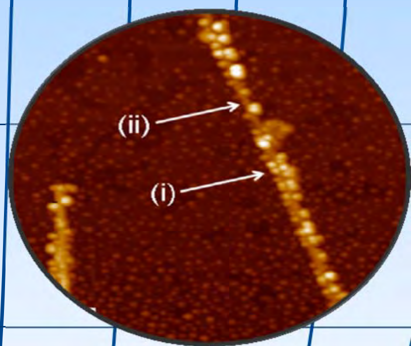

Very Simple Ultrashort Pulse Waveform Measurement and Reconstruction System

Prof. Tsuyoshi KONISHI(Osaka University)

1. Ultrashort Pulse Technology Load Map

- Simple Evaluation Technique is needed for widespread use.

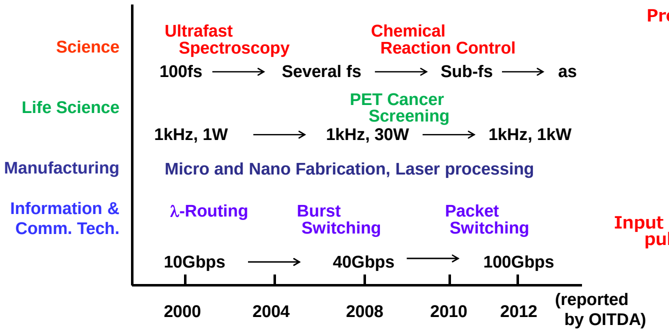

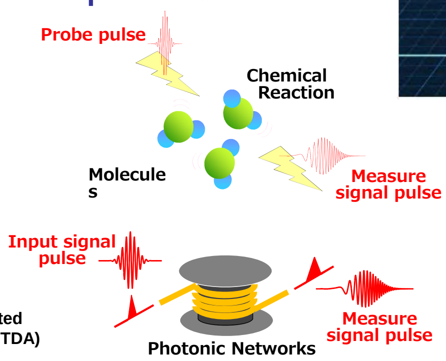

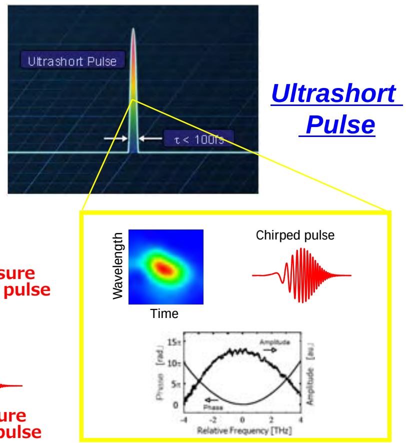

2. Comparison of conventional Measurement technique of Ultrashort pulse

	This Technique	Auto Correlator	SHG-FROG
Measurement Time	◎ Almost Real Time	◎ Real Time	△ ~ 10 min.
Phase Retrieval	○	×	○
Ease of Handling	◎	◎	△
Sensitivity	○ fJ~mJ	○ fJ~mJ	○ fJ~mJ

- A spectrometer is a simple and popular tool compared with commonly used measurement tools of ultrashort pulses.
- However, a spectrometer is not able to retrieve phase information of ultrashort pulses.

Our spectrometer-based approach allows retrieve phase information by using intensity-dependent spectral change and optimization algorithm.

3. Measurement and Reconstruction of Ultrashort pulse waveform

- System configuration

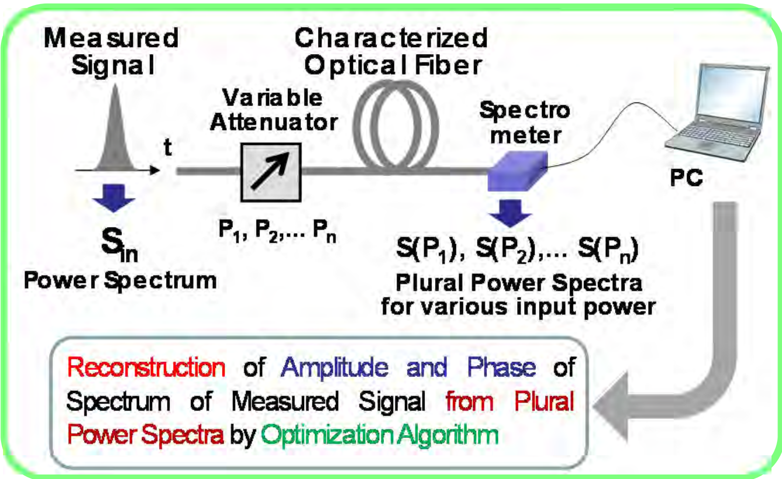

- Reconstructed Data and Its Accuracy

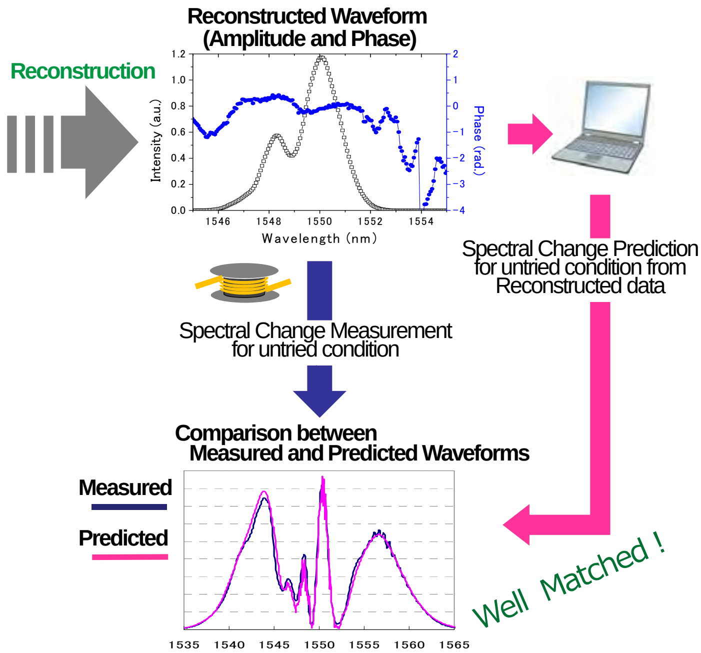

Detail of Procedure

1. Measurement of power spectra $S(P_1)$ ~$S(P_n)$ for various input powers by a Spectrometer.
2. Simulation of spectral change by propagation of an input optical signal through an optical fiber.
3. Optimization of input ultrashort pulse waveform so that difference in value between the calculated and measured power spectra will be minimized.

4. Patent available for licensing

Patent No. : US2011-311223, JP2009-48608 (US, JP)

Contact : Hisahiro MORIUCHI (JST)
phone:+81-3-5214-8486
e-mail: license@jst.go.jp

New Pump-probe Technique providing A Wide Range Time-scale and Nanoscale Measurement

Prof. Hidemi SHIGEKAWA (University of Tsukuba)

1. New Pump-probe Technique

● **Delay time modulation femtosecond time-resolved scanning probe microscope**

1. **Wide-time range measurement (femtosec. – microse.)**
2. **Overcome of the thermal effect**
3. **Temporal resolution determined by pulse width and spatial resolution determined by STM**

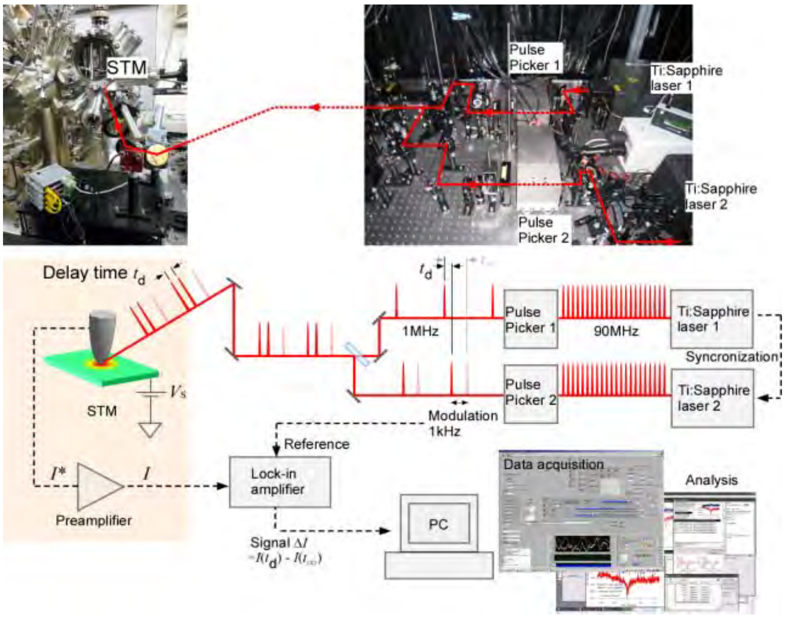

2. New key method

● Delay-time modulation

•Delay time is controlled in a digital form using pulse pickers.

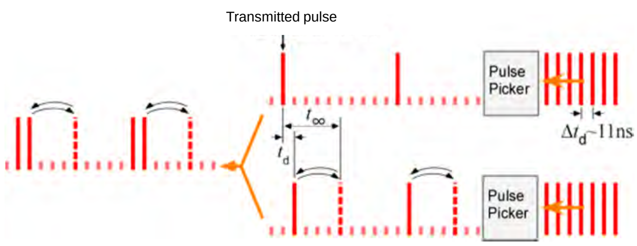

●Lock-in measurement

•Delay time t_d is modulated between t_{d1} (measurement point) and a large value of t_{d2}. The signal S(t_d) is measured by lock-in detection technique.

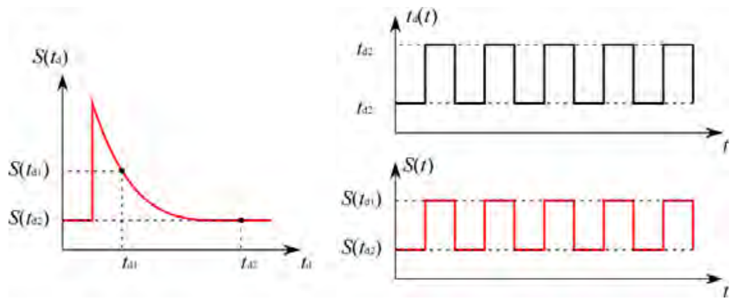

3. Measurement Examples

Real space imaging of transient carrier dynamics in the nanostructures with a wide variety of lifetimes

●Carrier lifetimes measured by STM

•Time-dependent STM signals can be obtained for various materials, providing the decay times of photoexcited carriers.

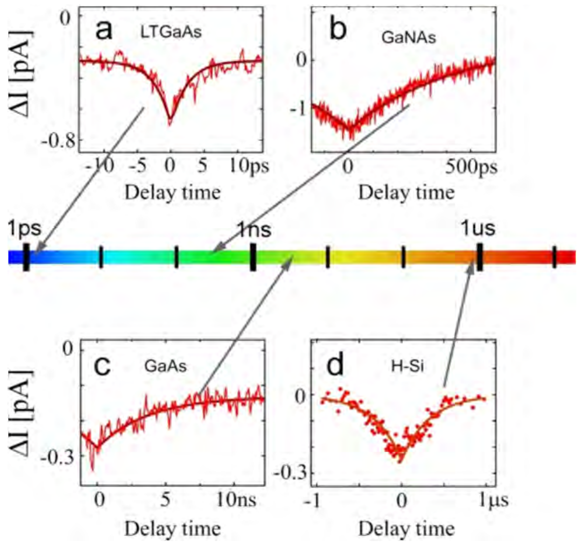

●Imaging nanoscale carrier dynamics

•Observation of diffusion and drift on carrier recombination processes in an inner potential of GaAs PIN structure

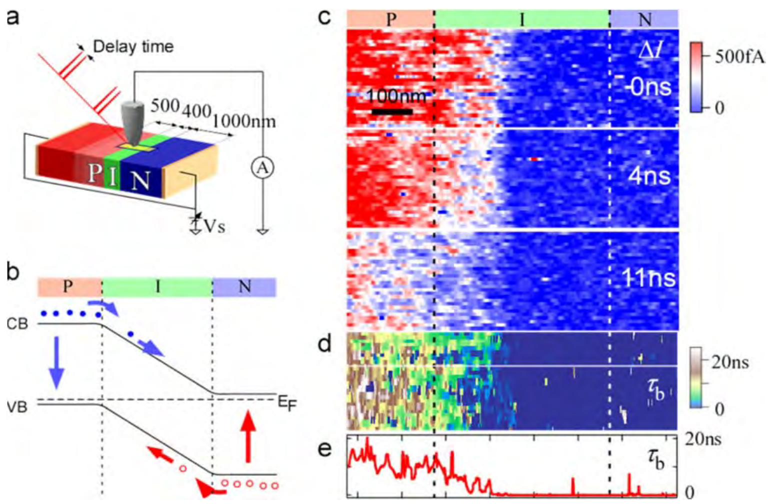

4. Patent for licensing

Patent No. : (1) WO/2008/066090, (2) WO/2003/046519 ((1) JP,US,EP,CA,CN,KR (2) JP,US,EP)

Contact : Hisahiro MORIUCHI (JST)
phone :+81-3-5214-8486
e-mail: license@jst.go.jp

Nano-suit: A Thin-layer of Amphiphilic Solution to Observe the Fine Structure of Living Organisms in FE-SEM

Dr. Takahiko HARIYAMA (Hamamatsu University School of Medicine)

1. We can observe living and moving specimens with SEM

(1) Various complex procedures with fixing tissues have precluded the real fine structure of organisms by a field emission scanning electron microscope.

(2) Here we present a new method to observe living organisms; their surfaces were covered with thin-layers of amphiphilic solution.

(3) Our method permits the use of a high vacuum (10^{-4}〜10^{-7}Pa) and achieves fine structural observations on live specimens.

2. Procedure

Animals : Larvae of the northern house mosquito, *Culex pipiens molestus*.

Treatment: Animals were dipped into amphiphilic solution blotted briefly on a dry filter paper to remove excess solution.

SEM observation: Mosquito larvae tolerated the high vacuum well. They continued to actively move around for 30 min under the SEM.

3. Electron micrograph of mosquito larvae

untreated

treated

traditional preparation

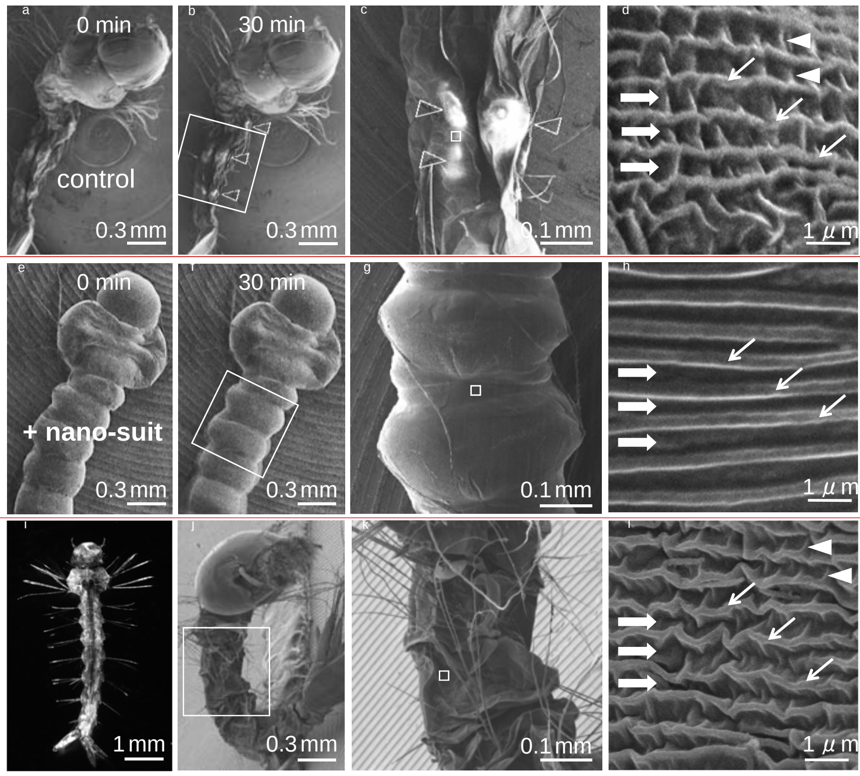

・Untreated larvae quickly shrank and ceased to move under SEM observation (Fig. a-d). There are many wrinkles in the furrows in the two control treatments (Fig. d, l).

・Treated larvae formed a nano-suit, showed rapid movements during 30±10min of SEM observation and suffered no observable morphological change (Fig. e-g). There are no wrinkles in the treated specimen (Fig. h).

・The artificial ECS (extra cellular substances) played a significant role as an extra barrier ameliorating the effects of high vacuum.

4. Patent available for licensing

Patent contact details: Yoshihiro MURAI (JST)
phone:+81-3-5214-8486
e-mail:licence@jst.go.jp

Patent No. : PCT/JP2012/72982
Inventors: Takahiko Hariyama, Masatsugu Shimomura, Yoshinori Muranaka, Hiroshi Suzuki, Yasuharu Takaku, Isao Ohta, Daisuke Ishii, Yuji Hirai

NanoTester : PCI-AFM

(Point-contact Current Imaging Atomic Force Microscopy)

Prof. Takuya MATSUMOTO (Osaka University)

1. NanoTester : PCI-AFM

PROBLEMS

of exisiting technologies for measuring nanoscale conductance

Contact mode?

○Easy operation

×Degradation of tip and sample

Tapping mode?

○High resolution

×insufficient electrical *contact*

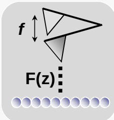

Point contact?

○Good electrical contact

×Mispositioning due to thermal drift

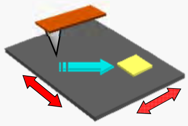

NOVEL TECHNOLOGY "PCI-AFM"

Enables *simultaneous nano-scale observation* of *topography and current image* for *biomaterials and soft materials*

Tapping mode
High resolution topography

\+

Point contact
Stable current-voltage curve measurement

Dynamically switched operation

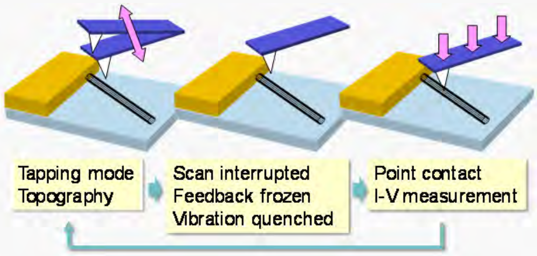

- **Drift free**
  : Simultaneous acquisition of topography & Current image
- **High speed measurement**
  : 128 X 128 points/10 min
- **High sensitivity** : 100GΩ (10pA)
- **Independent loading force setting**
  : Tapping mode (topography) / point contact (current detection)

2. Applications

Carbon Nanotube / Porphyrin Complex

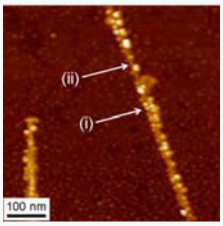

CNT / BPP-Zn complex

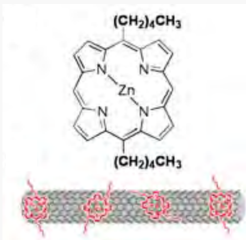

BPP-Zn
(5,15-bispentylporphyrinato zinc(II))

PCI-AFM successfully characterizes the π-Interface between nanotube and molecular system.

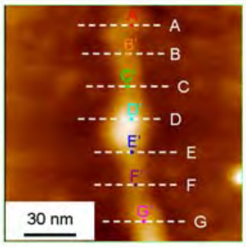

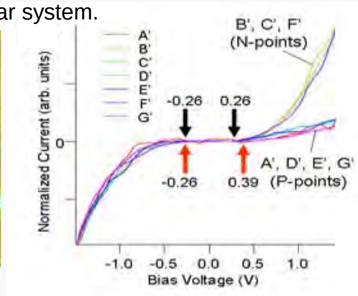

Application No.4

DNA

Topography

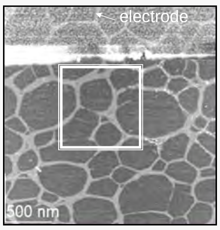

PCI-AFM 15% humidity

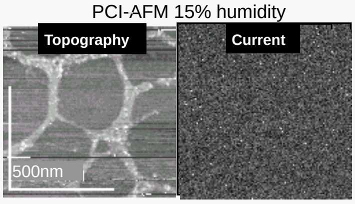

PCI-AFM 60% humidity

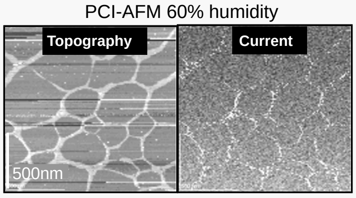

Application No.5

Charge Transfer Complex

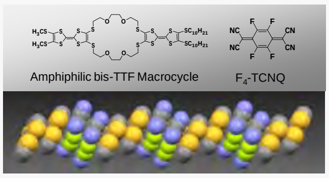

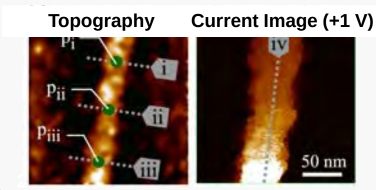

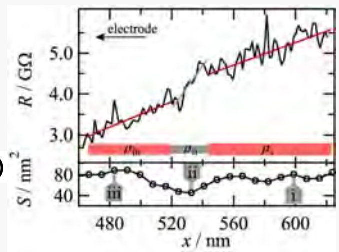

Application No.8

3. Patent available for licensing

Patent No. : US7,088,120, CA2503957 (US, CA)

Contact : Miho OKISHIRO (JST)
phone: +81-3-5214-8486
e-mail: license@jst.go.jp

PCI-AFM Applications

1. Instrumentation: *Jpn. J. Appl. Phys.* **41**, L742-L744 (2002)
2. Carbon nanotube: *Appl. Phys. Lett.* **82**, 1944-1946 (2003)
3. SAM: *Jpn. J. Appl. Phys.*, **43**, 4511-4516 (2004)
4. Porphyrin/ Carbon nanotube: *Adv. Mater.* **18**, 1411 (2006)
5. DNA network: *Appl. Phys. Lett.* **86**, 113901-113903 (2005)
6. Pb-phthalocyanine nanocrystal: submitted.
7. Tip control methods: *Nanotechnology* **18**, 095501 (2007)
8. Charge transfer complex: *Appl. Phys. Lett.* **93,** 173102 (2008)

Direction-Free Magnetic Field Application System

Dr. Ken HARADA (Hitachi Ltd.)

1. Necessity of direction-free magnetic application system

- **Objective : To observe the magnetic structure in materials by TEM using the techniques of**
  1) Lorentz microscopy
  2) electron holography

- **System architecture:**
  1) TEM + 2) Direction-free magnetic application system (New!)
  Applying external magnetic field to the specimen
  1) from an arbitrary direction
  2) with an arbitrary magnitude
  3) compensating the electron beam to the optical axis directly

2. Real implementation of the direction-free magnetic field application system

Ray diagram

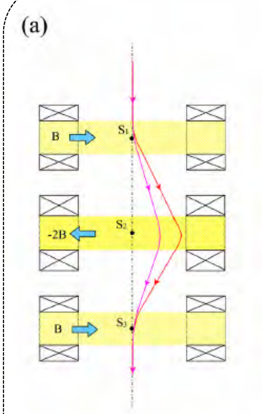

(a) Conventional three-step-type system

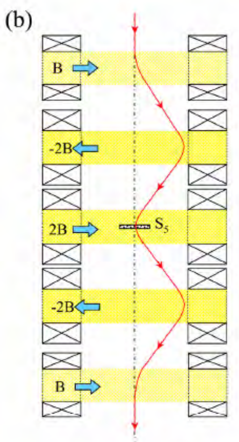

(b) Developed five-step-type system

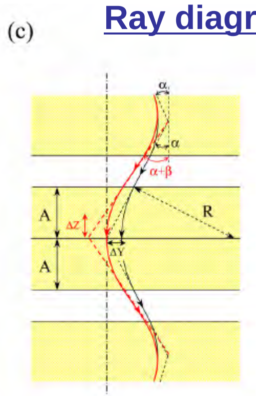

(c) Schematic of explanation of how to pass the specimen position S5 parallel to the optical axis by five-step-type

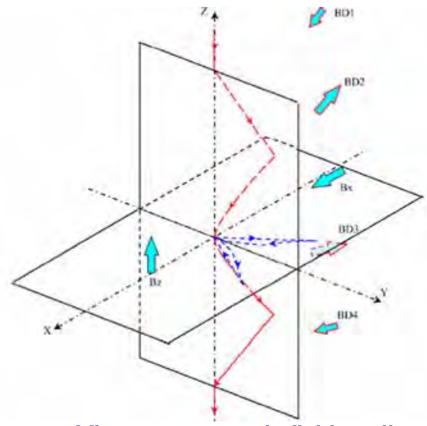

Ray diagram of five-step magnetic field application system within horizontal and vertical magnetic fields applied simultaneously.

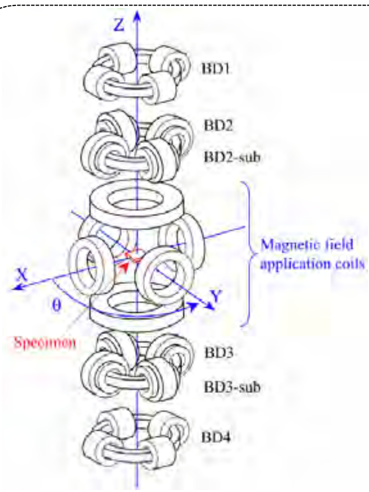

Schematic drawing of direction-free magnetic field application system.

Manufactured direction-free magnetic field application system (cut-model).

3. Observed image

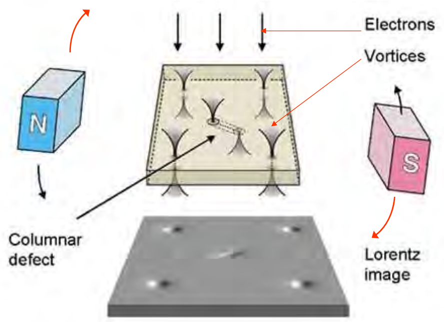

Experimental setup of Lorentz microscopy

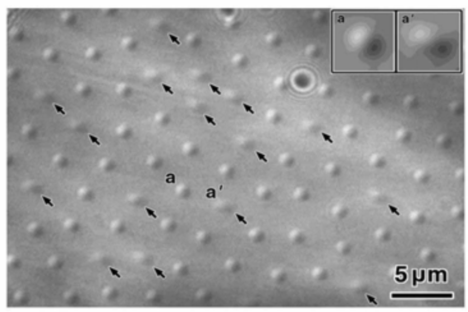

A Lorentz micrograph of $Bi_2Sr_2CaCu_2O_{8+\delta}$ (Bi-2212) thin film. Black and white contrast pairs are individual vortices trapped by columnar defects. The image of the perpendicular vortex lines are circular, whereas those of the tilted vortex lines pointed by black arrows are elongated and have lower contrast.

4. Patent available for licensing

Patent No. : US 6838675, EP 1376649
(US, EP(UK, DE, NL))

Contact : Takuji OHINATA (JST)
phone:+81-3-5214-8486
e-mail: license@jst.go.jp

About JST

The Japan Science and Technology Agency (JST) is one of the core institutions responsible for the implementation of science and technology policy in Japan, including the government's Science and Technology Basic Plan. From knowledge creation—the wellspring of innovation—to ensuring that the fruits of research are shared with society and Japan's citizens, JST undertakes its mission in a comprehensive manner. JST also works to provide a sound infrastructure of science and technology information and raise awareness and understanding of science and technology-related issues in Japan.

Mission :
We contribute to the creation of innovation in science and technology as the core implementing agency of the fourth phase of the Science and Technology Basic Plan.

Visions :
1.To achieve innovation in science and technology through creative research and development.
2.To maximize research outcomes by managing research resources on the virtual network.
3.To develop the nation's infrastructure for science and technology to accelerate innovation in science and technology.

http://www.jst.go.jp/EN/about/index.html

To Realize Benefits for the Whole of Society from Research Output

Japan Science and Technology Agency

Center for Intellectual Property Strategies

5-3, Yonbancho, Chiyoda-ku, Tokyo, 102-8666 JAPAN

Phone : +81-3-5214-8486

fax : +81-3-5214-8417

e-mail : license@jst.go.jp

URL : http://www.jst.go.jp/tt/EN/

http://www.jst.go.jp/tt/EN/mrs2012.html